

Figure 1 Phylogenetic tree construct of the partial S genome segment from patient samples. SS: S segment; SR-11: Seoul virus; THAIV: Thailand virus; HTNV: Hantaan virus; TPMV: Thotapalayam virus; 1, 2, 3, 4 and 5 represent the partial S segment from patient samples.

In this study, the mean number of days post onset of illness at which hantavirus RNA was detectable was 9 days (Table 1). One patient (#19) who was positive for hantavirus RNA had very low levels of second round product and the products could not be sequenced. In the remaining five patient samples that were positive for hantavirus RNA, the PCR products after a nested RT-PCR were sequenced and a phylogenetic tree was constructed. The nucleotide sequences were compared with S genome sequences of HTNV, SEOV, THAIV and TPMV. The phylogenetic analyses of the sequences are shown in Figure 1. The nucleotide identity of human sequences with that of HTNV ranged from 84% to 98.5%, with SEOV from 69% to 78.5%, with THAIV from 61% to 71.7% and with TPMV from 8.2% to 30%. The highest homology of the human sequences was with HTNV. Among the sequences from patient samples there was a nucleotide homology of 84–98.5%. Figure 2 shows the seasonal distribution of hantavirus cases in our

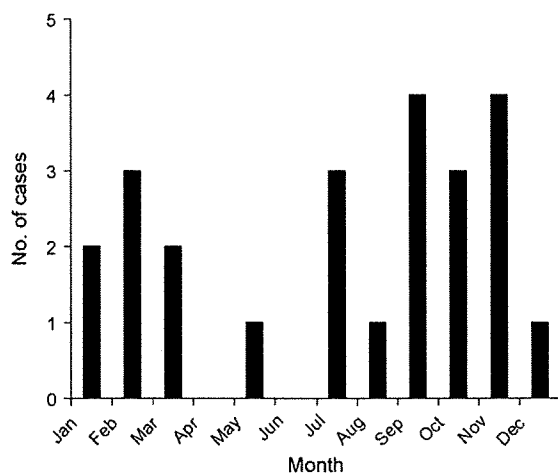


Figure 2 Cumulative seasonal distribution of hantavirus cases during 2005–2007, showing clustering of hantavirus cases in the early and latter part of the year.

study. Most of the cases were distributed in the early (spring) cool months and later (autumn) rainy months of the year.

4. Discussion

HFRS remains undefined in South Asia largely due to the unavailability of sensitive and specific serodiagnostic assays. IFAs and ELISA systems employing recombinant antigens are widely used. Hantavirus RNAemia is short lived and in some cases undetectable, thus the use of RT-PCR for hantavirus diagnosis is limited. Whatever the diagnostic tools used, reliability of results is an issue in areas where the circulating serotypes are largely unknown, hantavirus cases have not been documented and the extent of hantavirus-related disease is unknown. The present study was performed to expand our knowledge of hantavirus-related acute febrile illness in India and to advocate judicious use of serological and molecular techniques to improve hantavirus diagnosis.

Serological assays for hantavirus diagnosis in India should include antigens of HTNV, DOBV, PUUV and TPMV as several distinct hantaviruses cause HFRS in the Old World. Serology based on IgM ELISA is effective in the rapid diagnosis of hantavirus infections in endemic regions of the world.

In this study, 78 patients (22.5%) tested positive for anti-hantavirus IgM by ELISA and IFA, only 18 of whom had detectable levels of hantavirus-specific IgG. Although the demonstration of both IgM and IgG hantavirus-specific antibodies enables reliable serological confirmation of hantavirus infection, immune responses could differ with the infecting hantavirus serotype. Delayed IgM response in nephropathia epidemica (NE) has been reported and in approximately 5–10% of NE patients detectable levels of IgG were not seen at the time of admission.¹⁹ In the absence of a μ -capture ELISA, stringent serological criteria such as those adopted in this study have the limitation of missing cases with a delayed IgM/IgG response. This would also explain the absence of anti-hantavirus IgM in two patients who were positive for hantavirus RNA.

Differences in the type of antigens used in the assays (ELISA and IFA) and/or the circulation of unknown hantavirus serotypes in the region could explain the differences in reactivities seen in the two assays.

These molecular findings correlate well with results of a serotyping study which indicated that the circulating serotypes are predominantly HTNV-like as well as the presence of Thailand and a non-typeable Hantaan-like species in India. The reactivity pattern of serotyping appears to suggest the presence of more than a single novel hantavirus species in India (our unpublished data). However, these results are preliminary and a complete picture must await characterisation of circulating serotypes with primers designed to detect specific circulating serotypes/genotypes.

Sequences obtained from patients were very divergent from TPMV, the only documented serotype from India. At this juncture we would not be able to comment on these results as the divergence of TPMV from other hantaviruses warrants the use of novel serological and molecular assays for its detection.

There were a few limitations of this study. Owing to the unavailability of antigens, it was not possible to com-

pare the reactivity of samples with individual antigens of different serotypes, which would have given a better picture of the circulating serotype. The size of the second round product was small and novel primers for larger amplicons await design. We could not obtain convalescent sera from most of the patients. TPMV is an important isolate from India and needs to be included in serological panels, as cross-reactivity between TPMV and other hantaviruses is reportedly low.

Approximately 20% of acute HFRS cases are positive for hantavirus RNA²⁰ and thus molecular diagnosis should be used only to complement serodiagnostic assays. RT-PCR may show false negativity as the viraemia in hantavirus infections is short. Most of the patients with febrile illness attending our clinics seek medical care around a week after the onset of illness. Samples are best suited for demonstration of hantavirus RNA when collected within 5–7 days after the onset of illness.

All infectious agents carried by rodents or ectoparasites of rodents should be considered in tandem. Co-infection with *Leptospira* and hantavirus has been reported.²¹ In our study, three patients showed co-infection with hantavirus and leptospirosis whilst two were co-infected with dengue and hantavirus.

The temporal distribution of cases can also be correlated with the distribution of seasonal fluctuations in rodent populations in India. In South Asia, some of the bandicoot (giant rat) species (genus *Bandicota*) have two peaks in breeding activity (April and August–September²²) and population densities of rats as documented are greatest from September–November and lowest from May–July.²³

This study complements our previous reports on hantavirus activity in India. It establishes the likelihood of hantavirus infections among patients with acute febrile illness. Since the clinical features of hantavirus infections are not pathognomonic and laboratory work-up is essential for confirmation of the diagnosis, it is important to establish cost-effective, user-friendly diagnostic tools (serological and molecular) for rapid diagnosis of hantavirus infections in humans.

Authors' contributions: GS and PA designed the study protocol; SC carried out the immunoassays and drafted the manuscript; KY and JA supplied IFA slides and helped analyse the results obtained; HKB, AC, KT and AP carried out the clinical assessment, with the identification of subjects and collection of samples. All authors read and approved the final manuscript. GS is guarantor of the paper.

Acknowledgement: The authors acknowledge the contribution of Dr Connie Schmaljohn of the United States Army Medical Research Institute of Infectious Diseases (USAMRIID), Fort Detrick, MD, USA, in supplying cDNA of the S segment of HTNV and SEOV as positive controls for molecular studies.

Funding: This study was jointly funded by intramural research funds of the Christian Medical College, Vellore, Tamil Nadu, India (R.C. Min. No. 5115 dated March 2003) and by a grant from the Indian Council for Medical Research (ICMR), New Delhi, India (Reference No./DO. No. 5/8/7/23/2004-ECD-1).

Conflicts of interest: None declared.

Ethical approval: Institutional Research Ethics Committee of the Christian Medical College, Vellore, Tamil Nadu, India (R.C. Min. No. 5838 dated 21 February 2006) and the Indian Council for Medical Research (ICMR).

Appendix A. Supplementary data

Supplementary data associated with this article can be found, in the online version, at doi:10.1016/j.trstmh.2009.01.016.

References

- Evander M, Eriksson I, Pettersson L, Joto P, Ahlm C, Olsson GE, et al. Puumala hantavirus viremia diagnosed by real-time reverse transcriptase PCR using samples from patients with hemorrhagic fever and renal syndrome. *J Clin Microbiol* 2007;45:2491–7.
- Schmaljohn C, Hjelle B. Hantaviruses: a global disease problem. *Emerg Infect Dis* 1997;3:95–104.
- Krüger DH, Ulrich R, Lundkvist AA. Hantavirus infections and their prevention. *Microbes Infect* 2001;3:1129–44.
- Lednicky JA. Hantaviruses. A short review. *Arch Pathol Lab Med* 2003;127:30–5.
- Severson W, Xu X, Kuhn M, Senutovitch N, Thokala M, Ferron F, et al. Essential amino acids of the Hantaan virus N protein in its interaction with RNA. *J Virol* 2005;79:10032–9.
- Carey DE, Reuben R, Panicker KN, Shope RE, Myers RM. Thottapalayam virus: a presumptive arbovirus isolated from a shrew in India. *Indian J Med Res* 1971;59:1758–60.
- Wichmann D, Slenczka W, Alter P, Boehm S, Feldmann H. Hemorrhagic fever with renal syndrome: diagnostic problems with a known disease. *J Clin Microbiol* 2001;39:3414–6.
- Bruno P, Hassel LH, Brown J, Tanner W, Lau A. The protean manifestations of hemorrhagic fever with renal syndrome. A retrospective review of 26 cases from Korea. *Ann Intern Med* 1990;113:385–91.
- Schilling S, Emmerich P, Klempa B, Auste B, Schnaith E, Schmitz H, et al. Hantavirus disease outbreak in Germany: limitations of routine serological diagnostics and clustering of virus sequences of human and rodent origin. *J Clin Microbiol* 2007;45:3008–14.
- Vapalahti O, Lundkvist A, Kallio-kokko H, Paukku K, Julkunen I, Lankinen H, et al. Antigenic properties and diagnostic potential of puumala virus nucleocapsid protein expressed in insect cells. *J Clin Microbiol* 1996;34:119–25.
- Hujakka H, Koistinen V, Kuronen I, Eerikainen P, Parviainen M, Lundkvist A, et al. Diagnostic rapid tests for acute hantavirus infections: specific tests for Hantaan, Dobrava and Puumala viruses versus a hantavirus combination test. *J Virol Methods* 2003;108:117–22.
- Arthur RR, Lofts RS, Gomez J, Glass GE, Leduc JW, Childs JE. Grouping of hantaviruses by small (S) genome segment polymerase chain reaction and amplification of viral RNA from wild-caught rats. *Am J Trop Med Hyg* 1992;47:210–24.
- Xiao SY, Chu YK, Knauert FK, Lofts R, Dalrymple JM, LeDuc JW. Comparison of hantavirus isolates using a genus-reactive primer pair polymerase chain reaction. *J Gen Virol* 1992;73:567–73.
- Khaiboullina SF, Morzunov SP, St Jeor SC. Hantaviruses: molecular biology, evolution and pathogenesis. *Curr Mol Med* 2005;5:773–90.

15. Raboni SM, Rubio G, De Borba L, Zeferino A, Skraba I, Goldenberg S, et al. Clinical survey of hantavirus in southern Brazil and the development of specific molecular diagnostic tools. *Am J Trop Med Hyg* 2005;72:800–4.
16. McCaughey C, Hart CA. Hantaviruses. *J Med Microbiol* 2000;49:587–99.
17. Chandy S, Mitra S, Sathish N, Vijayakumar TS, Abraham OC, Jesudason MV, et al. A pilot study for serological evidence of hantavirus infection in human population in south India. *Indian J Med Res* 2005;122:211–5.
18. Chandy S, Yoshimatsu K, Ulrich RG, Mertens M, Okumura M, Rajendran P, et al. Seroepidemiological study on hantavirus infections in India. *Trans R Soc Trop Med Hyg* 2008;102:70–4.
19. Lundkvist A, Bjorsten S, Niklasson B, Ahlborg N. Mapping of B-cell determinants in the nucleocapsid protein of Puumala virus: definition of epitopes specific for acute immunoglobulin G recognition in humans. *Clin Diagn Lab Immunol* 1995;2:82–6.
20. Miyamoto H, Kariwa H, Araki K, Lokugamage K, Hayasaka D, Cui BZ. Serological analysis of hemorrhagic fever with renal syndrome (HFRS) patients in Far Eastern Russia and identification of the causative hantavirus genotype. *Arch Virol* 2003;148:1543–56.
21. Markotic A, Kuzman I, Babic K, Gagro A, Nichol S, Ksiasek TG, et al. Double trouble: hemorrhagic fever with renal syndrome and leptospirosis. *Scand J Infect Dis* 2001;34:221–4.
22. Hussain I, Cheema AM, Khan AA. Small rodents in the crop ecosystem of Pothwar Plateau, Pakistan. *Wildl Res* 2000;30:269–74.
23. Srihari K, Govinda RK. Effective period for control of *Bandicota bengalensis* in paddy fields. *Trop Pest Manage* 1998;34:141–6.

Coxiella burnetii Isolates Cause Genogroup-Specific Virulence in Mouse and Guinea Pig Models of Acute Q Fever[†]

K. E. Russell-Lodrigue,^{1,3,‡} M. Andoh,^{1,‡} M. W. J. Poels,^{1,2} H. R. Shive,³ B. R. Weeks,³ G. Q. Zhang,¹ C. Tersteeg,^{1,2} T. Masegi,⁴ A. Hotta,⁵ T. Yamaguchi,⁵ H. Fukushi,⁵ K. Hirai,⁵ D. N. McMurray,¹ and J. E. Samuel^{1,*}

Department of Microbial and Molecular Pathogenesis, Texas A&M Health Science Center, College Station, Texas¹; Institute of Life Sciences and Chemistry, Utrecht, The Netherlands²; Department of Veterinary Pathobiology, Texas A&M University, College Station, Texas³; and Department of Pathogenetic Veterinary Science⁴ and Department of Applied Veterinary Science,⁵ United Graduate School of Veterinary Sciences, Gifu University, Gifu, Japan

Received 28 July 2009/Returned for modification 13 August 2009/Accepted 18 September 2009

Q fever is a zoonotic disease of worldwide significance caused by the obligate intracellular bacterium *Coxiella burnetii*. Humans with Q fever may experience an acute flu-like illness and pneumonia and/or chronic hepatitis or endocarditis. Various markers demonstrate significant phylogenetic separation between and clustering among isolates from acute and chronic human disease. The clinical and pathological responses to infection with phase I *C. burnetii* isolates from the following four genomic groups were evaluated in immunocompetent and immunocompromised mice and in guinea pig infection models: group I (Nine Mile, African, and Ohio), group IV (Priscilla and P), group V (G and S), and group VI (Dugway). Isolates from all of the groups produced disease in the SCID mouse model, and genogroup-consistent trends were noted in cytokine production in response to infection in the immunocompetent-mouse model. Guinea pigs developed severe acute disease when aerosol challenged with group I isolates, mild to moderate acute disease in response to group V isolates, and no acute disease when infected with group IV and VI isolates. *C. burnetii* isolates have a range of disease potentials; isolates within the same genomic group cause similar pathological responses, and there is a clear distinction in strain virulence between these genomic groups.

Coxiella burnetii, the etiologic agent of acute and chronic Q fever, is an obligate intracellular bacterium with worldwide distribution and a diverse host range. Livestock serve as the organism's primary reservoir and may be asymptomatic carriers or exhibit reproductive disorders. Ticks are important in the maintenance of the disease in nature and have been shown to transmit the infection transovarially (37). Humans are most often infected through inhalation of the bacterium in fine-particle aerosols, though transmission may also occur through ingestion of the organism from contaminated, unpasteurized dairy products (22, 27). Although a high percentage of infections may result in subclinical or asymptomatic infection, humans can become ill from exposure to as few as 10 organisms (6) and may display signs of (i) an acute flu-like illness with or without pneumonia and/or hepatitis (30, 31) or (ii) a chronic disease manifesting most frequently as endocarditis and/or hepatitis (40, 41).

C. burnetii isolates have been obtained from natural Q fever infections in humans and other animals. Several theories have been proposed to explain the dichotomy in development of acute and chronic Q fever. Unique sequence differences between genomic groups are correlated with the clinical expres-

sion of Q fever (44). Biochemical markers have grouped *C. burnetii* isolates from chronic-disease patients separately from acute-disease/arthropod/domestic animal isolates, but whether these groupings predict virulence potential and acute/chronic-disease outcomes has not yet been fully resolved (20). Samuel et al. were the first to separate these isolates and their resulting diseases based on plasmid patterns (44). Hackstadt used variations in lipopolysaccharide (LPS) banding patterns to divide isolates of *C. burnetii* into three groups, and group distinction was noted in correlation with acute or chronic disease (16). Hendrix et al. separated *C. burnetii* isolates into six genomic groups (20). Group I to III isolates have a QpH1 plasmid and have been isolated from ticks, acute human Q fever cases, cow's milk, and livestock abortions. Groups IV and V have a QpRS plasmid or no plasmid (with plasmid-related sequences integrated into the chromosome), respectively, and have been associated with livestock abortions and human chronic endocarditis or hepatitis. Group VI isolates were collected from wild rodents in Dugway, UT, and were infectious but avirulent in rodent models of disease (47, 48). Jager et al. used restriction fragment length polymorphism (RFLP) to differentiate 80 *C. burnetii* isolates and reproduced distinguishable patterns for reference isolates in groups I, IV, V, and VI (23). More recently, multiple-locus variable nucleotide tandem repeat analyses (49) have validated these groupings. Infrequent-restriction-site PCR of 14 livestock and tick isolates resulted in six groups; subsequent multiple-locus variable-number tandem repeat analysis typing of 42 isolates revealed 36 genotypes (2). Glazunova et al. used multispacer sequence typing to analyze 173 isolates, a majority of which were acquired from chronic-

* Corresponding author. Mailing address: Department of Microbial and Molecular Pathogenesis, Texas A&M Health Science Center, College Station, TX 77843-1114. Phone: (979) 862-1684. Fax: (979) 845-3479. E-mail: jsamuel@medicine.tamhsc.edu.

† Supplemental material for this article may be found at <http://iai.asm.org/>.

‡ K.E.R.-L. and M.A. contributed equally to this work.

§ Published ahead of print on 28 September 2009.

TABLE 1. Isolates evaluated for virulence

Genomic group	Isolate	Notation in this study	Original source			
			Sample	Yr	Location	Disease
I	Nine Mile RSA493	NM	Tick	1935	Montana, US	NA ^a (acute; flu-like in humans)
	African RSA334	African	Human blood	1949	Central Africa	Acute; Congolese Red Fever
	Ohio 314 RSA270	Ohio	Cow's milk	1956	Ohio, US	Persistent
IV	MSU Goat Q177	Priscilla	Goat Cotyledon	1980	Montana, US	Abortion
	P Q173	P	Human heart valve	1979	California, US	Endocarditis
V	G Q212	G	Human heart valve	1981	Nova Scotia, Canada	Endocarditis
	S Q217	S	Human liver biopsy specimen	1981	Montana, US	Hepatitis
VI	Dugway 5J108-111	Dugway	Rodents	1958	Utah, US	NA

^a NA, not applicable.

disease patients, and identified 30 genotypes in three monophyletic groups; an association between the plasmid type, some genotypes, and the nature of disease was observed (15). These monophyletic groups supported the early RFLP groups and placed groups I, II, and III in one monophyletic group; group IV in the second monophyletic group; and group V in the third monophyletic group. A comprehensive microarray-based whole-genome comparison by Beare et al. confirmed the relatedness of RFLP-grouped isolates and added two more genomic groups, VII and VIII (4). Differences in novel gene contents and pseudogenes may be factors in the variations in virulence seen among group I, IV, V, and VI isolates (5). It has been shown in an intraperitoneal (i.p.)-challenge guinea pig model that 10^1 organisms of the acute-disease-associated group I isolate Nine Mile RSA493 (NM) caused fever, but 10^6 chronic-disease-associated group IV isolate MSU Goat Q177 (Priscilla) organisms were required to induce fever (36).

In opposition to the theory of genotype/pathotype correlation, Stein and Raoult evaluated 28 human isolates and found that isolates bearing the QpH1 plasmid were present in both acute and chronic Q fever patients in France and that isolates without the QpH1 plasmid were able to cause acute disease (46). QpH1 plasmid-containing isolates have also been isolated from chronic-endocarditis patients (50). Several groups have speculated that host factors are primarily responsible for the outcome of infection with *C. burnetii*. Individual differences in immune function lead to varying sensitivity to infection and disease development. In this model, acute and chronic disease could be caused by organisms from the same isolate group, and chronic disease could develop because of compromised resistance of the host rather than as a consequence of a specific property of the pathogen. For example, human immunodeficiency virus infection is a risk factor for the development of chronic Q fever endocarditis (9, 29). Deficiencies in the host-specific cell-mediated immune response in Q fever patients have been associated with the suppression of monocyte and macrophage activities (25), and monocytes from chronic-Q fever patients have been shown to be defective in phagosome maturation and to have impaired *C. burnetii*-killing potential, regulated in part by elevated interleukin-10 (IL-10) expression (14). There is strong clinical evidence to support the role of increased host production of IL-10 in the development of both Q fever endocarditis and chronic fatigue syndrome (11, 12, 21, 39). A recent study suggested that chronic Q fever endocarditis may be associated with atypical M2 polarization and stimula-

tion of bacterial replication (7), but the pathogenic process that mediates this polarization was undefined.

The route of infection may also be an important determining factor in the manifestation of acute and chronic Q fever. La Scola et al. and Marrie et al. demonstrated that the route of infection and the size of the inoculum affected clinical illness and pathology associated with infection in mouse and guinea pig models (26, 33). Differences in the geographic distributions of the diseases have also been noted (32); in Nova Scotia, for example, the primary manifestation of acute Q fever is pneumonia (34), but in France it is hepatitis, possibly due to ingestion of raw milk and unpasteurized cheeses (51).

The pathogenicity of *C. burnetii* has been evaluated using guinea pigs, mice, and chicken embryos. Febrile response, splenomegaly, and mortality in guinea pigs; splenomegaly and mortality in mice; and mortality in chicken embryos are indicators of virulence for *C. burnetii*. The establishment of an aerosol model of *C. burnetii* infection in guinea pigs (43) provides a relevant model in which to test isolate virulence. Additionally, severe combined immunodeficient (SCID) mice are highly sensitive to the *C. burnetii* prototype (NM isolate) (1), and the 50% lethal dose (LD_{50}) of NM in SCID mice was at least 10^8 times less than in wild type mice. We speculated that with these highly sensitive rodent models it may be possible to observe intra- and intergroup pathogenicity differences of *C. burnetii* isolates. To confirm whether SCID mice could be used to model isolate-specific virulence, we gave multiple infectious doses of a group IV Q fever isolate to immune-competent CB-17 and SCID mice (on the same background) to compare them with previously reported group I isolate (NM) infections (1). Eight isolates from four genomic groups (Table 1) were then evaluated for the ability to cause acute disease in SCID mouse i.p.-challenge and guinea pig aerosol challenge models. We hypothesized that isolates within the same genotypic group would cause similar diseases and that there would be a distinct difference in disease manifestations between isolate groups. Finally, we evaluated the potential of a vaccine composed of one *C. burnetii* isolate to protect guinea pigs against infection with an isolate from another group, since cross-protection between disparate isolate groups is a further indication of antigenic relatedness.

MATERIALS AND METHODS

Animals. The female 6- to 7-week-old CB-17/Icr-scid/scid (SCID) and wild-type CB-17/Icr^{+/+} (CB-17) mice used in Japan were purchased from Japan

CLEA (Tokyo, Japan); A/J mice were purchased from Japan SLC (Shizuoka, Japan). A/J mice were used because they are considered more susceptible to *C. burnetii* than other inbred mouse strains (45). The female 6- to 8-week-old SCID and wild-type CB-17 mice used in the United States were purchased from Taconic (Hudson, NY). Female Hartley guinea pigs weighing approximately 350 to 450 g were purchased from Charles River Laboratories (Wilmington, MA).

All infected animals were housed in approved animal biosafety level 3 facilities, and immunodeficient mice were housed under sterile conditions. All animals used in this study were acclimated to the facility and assessment procedures during the week prior to infection to decrease stress-related abnormalities. Animal health was assessed daily by a veterinarian.

Mouse experiments performed in Japan adhered to the guidelines for animal experiments at Gifu University. The Texas A&M University Laboratory Animal Care Committee reviewed and approved the mouse and guinea pig research at Texas A&M University, and experiments were carried out in AAALAC-approved facilities in accordance with university and federal regulations.

***C. burnetii*.** Eight *C. burnetii* isolates from four genomic groups (Table 1) were used. For the initial dose-effect experiment in Japan, *C. burnetii* MSU Goat Q177 (Priscilla), obtained from J. Kazar, Institute of Virology, Bratislava, Slovakia, was maintained in mice by passage in spleen homogenates at Gifu University. The spleen homogenates were stored at -80°C until they were used. The absence of contamination with other pathogens was confirmed by direct staining (Giménez and Gram staining), detection of *Mycoplasma* DNA using a PCR *Mycoplasma* detection set (Takara, Shiga, Japan), and inoculation of the spleen homogenate into cell culture and SCID mice (independent experimental infection from the study described here). The bacterial dose was evaluated as the 50% tissue culture infectious dose (TCID₅₀) in BGM cells (buffalo green monkey fibroblasts), the 50% infectious dose (ID₅₀) in CB-17 mice, and the LD₅₀ in SCID mice. The TCID₅₀ was determined by detecting the bacteria 6 days after infection using immunofluorescence staining with anti-*C. burnetii* rabbit antiserum. The ID₅₀ was determined by detecting seroconversion (immunoglobulin G [IgG], >1:16) using indirect microimmunofluorescence. The LD₅₀ was determined as reported previously (1).

For all subsequent experiments, all of the *C. burnetii* isolates were maintained at the Texas A&M Health Science Center. The *C. burnetii* isolates were cultivated in embryonated chicken eggs, purified by gradient centrifugation as previously reported (19, 44, 53), and stored at -80°C until they were used. The absence of contamination by other pathogens was confirmed as described above. *C. burnetii* was quantified by optical density (OD) (53), direct viable-particle count using the Live/Dead BacLight Bacterial Viability Kit (Molecular Probes, Eugene, OR), and quantitative real-time PCR (qPCR) using primers amplifying the *com1* gene (8) (see Table S1 in the supplemental material). The bacterial dose used for mouse infections was determined by qPCR; guinea pig doses were calculated using the OD.

Experimental infection in mice. (i) **Dose/effect experiment with the Priscilla isolate.** Six mice per group were used for the dose/effect experiment. SCID, CB-17, and A/J mice were inoculated i.p. with serial 10-fold dilutions of Priscilla (10^2 to 10^{-7} TCID₅₀ per animal) or sterile phosphate-buffered saline (PBS) (sham infection). SCID mice were observed for 112 days (16 weeks), and CB-17 and A/J mice were observed for 30 days.

(ii) **Genomic group comparison.** Four mice per group were used for the genomic group comparison. Each of eight *C. burnetii* isolates described in Table 1 (10^5 genome copies/animal) or PBS was administered i.p. to SCID and CB-17 mice. Two independent infections were performed, and the mice were observed for 28 days (for all of the *C. burnetii* isolates in SCID and CB-17 mice) or until death (for four representative *C. burnetii* isolates in SCID mice).

Clinical signs were evaluated every 2 days by visual observation (ruffled fur, hunched-back appearance, and lethargy) and body weight measurement. Body weight changes were evaluated using a body weight index (BWI) derived as follows: BWI = relative body weight/mean relative body weight of the control group; relative body weight = body weight on day "x" of infection/body weight on the day of infection. Cachexia was diagnosed when a mouse was lethargic and had a BWI of less than 0.85. At necropsy, the spleen weight was measured as an indicator of *C. burnetii* infection (54), and tissues were collected. To quantify the growth of *C. burnetii*, DNA was extracted from spleen tissue and *C. burnetii com1* gene copies were detected by qPCR as previously described (8). The heart, lung, liver, spleen, kidney, and femur were formalin fixed, embedded in paraffin, sliced, and then prepared by hematoxylin-eosin staining and immunocytochemistry, as described previously (1, 8), to evaluate histopathologic changes and bacterial distribution in tissues. The degree of inflammation present in each tissue sample was scored numerically by the following system: 0, none; 1, mild; 2, moderate; 3, marked; 4, severe. IgG titers for phase I and II *C. burnetii* in the sera of CB-17 mice were measured by microimmunofluorescence as described elsewhere (1).

For cytokine assays, blood was collected from the lateral saphenous vein at 3, 7, 10, 14, and 21 days postinfection (p.i.) and via cardiac puncture at 28 days p.i. after euthanasia, and the group pooled sera were stored at -80°C until they were used. Sixteen cytokines (IL-1 α , IL-1 β , IL-2, IL-3, IL-4, IL-5, IL-6, IL-12p40, IL-12p70, IL-10, granulocyte-macrophage colony-stimulating factor, gamma interferon [IFN- γ], KC, macrophage inflammatory protein 1 α [MIP-1 α], RANTES, and tumor necrosis factor alpha [TNF- α]) were measured using the Bio-Plex cytokine assay system (Bio-Rad, Hercules, CA) following the manufacturer's protocol. The cytokine quantification assay was performed in duplicate for each sample. The cytokine levels of infected sera were evaluated as the induction values compared to the values of uninfected sera.

Experimental infection in guinea pigs. A chamber specially designed to deliver droplet nuclei directly to the alveolar spaces (College of Engineering Shops, University of Wisconsin, Madison), allowing the infection of multiple guinea pigs simultaneously and ensuring uniform infection within each challenge group (35, 43, 52), was used for all guinea pig infection studies. (i) Three guinea pigs per group were infected with low (10^2), mid-level (10^4), or high (10^6) doses of one of the phase I *C. burnetii* isolates described in Table 1. Four negative control animals were sham infected with sterile PBS. Body weight, rectal temperature, and behavioral attitude were recorded, along with any abnormalities noted on thoracic auscultation and abdominal palpation. A rectal temperature of $\geq 39.5^{\circ}\text{C}$ was defined as fever. The guinea pigs were observed for 28 days p.i. The spleens and livers were weighed at necropsy. Tissues were collected and formalin fixed for histopathologic evaluation. Serum was obtained from each animal for serologic testing. (ii) In a separate experiment, three guinea pigs per group were exposed to PBS or 2×10^6 particle equivalents of NM, P, G, or Dugway. Daily assessment of these animals was performed as described above, and the organs were weighed at necropsy 14 days p.i. to detect splenomegaly and/or hepatomegaly. (iii) In the heterologous-protection study, guinea pigs were vaccinated twice with 40 μg of formalin-inactivated group I (NM) or group V (S) *C. burnetii* in Freund's incomplete adjuvant or with adjuvant alone, with 2-week intervals between the vaccinations and infection. The animals were then infected with high doses of either NM or S. Three animals per group were separated into the following six groups: (a) nonvaccinated, NM infected; (b) nonvaccinated, S infected; (c) NM vaccinated, NM infected; (d) S vaccinated, S infected; (e) NM vaccinated, S infected; and (f) S vaccinated, NM infected. The guinea pigs were monitored for 14 days p.i. for development of fever and other clinical signs of illness.

Histopathologic samples were prepared by hematoxylin and eosin staining or by immunohistochemistry using a Vectastain ABC kit and a Vector NovaRed substrate kit (Vector Laboratories, Burlingame, CA) and in-house-generated rabbit anti-*C. burnetii* NM (3) and by counterstaining them with hematoxylin. All slides were evaluated in a blinded fashion. Serum samples collected at necropsy were tested by enzyme-linked immunosorbent assay for IgG titers against phase I *C. burnetii* NM antigen as previously described (43). Sera from uninfected guinea pigs were used as negative controls.

Statistical analyses. The results were expressed as means for each group and were compared using one- and two-way analysis of variance or Student's *t* test, as appropriate. Differences were considered significant at a *P* value of <0.05 .

RESULTS

***C. burnetii* Priscilla is infective and exhibits delayed virulence in SCID mice.** A detailed analysis of dose-effect in an immunocompromised-mouse model supported the previous study by Moos and Hackstadt that evaluated the ability of the Priscilla isolate to cause fever in i.p.-challenged guinea pigs (36). The infectious titer of the Priscilla isolate in the splenic homogenate used for the multiple-dose infection was 2×10^4 TCID₅₀/ml in BGM cells, $2 \times 10^{9.3}$ ID₅₀/ml in CB-17 mice, and 2×10^{10} LD₅₀/ml in SCID mice (1 TCID₅₀ corresponded to $10^{5.3}$ ID₅₀ in CB-17 mice and to 10^6 LD₅₀ in SCID mice). The LD₅₀ in CB-17 mice could not be determined because no CB-17 mice died from any infectious dose used in this study, and the ID₅₀ in SCID mice could not be determined due to lack of antibody production. The ID₅₀ in CB-17 mice and the LD₅₀ in SCID mice were similar, suggesting that SCID mice could be lethally infected with very few viable organisms.

Multiple-dose infection of SCID mice with the Priscilla iso-

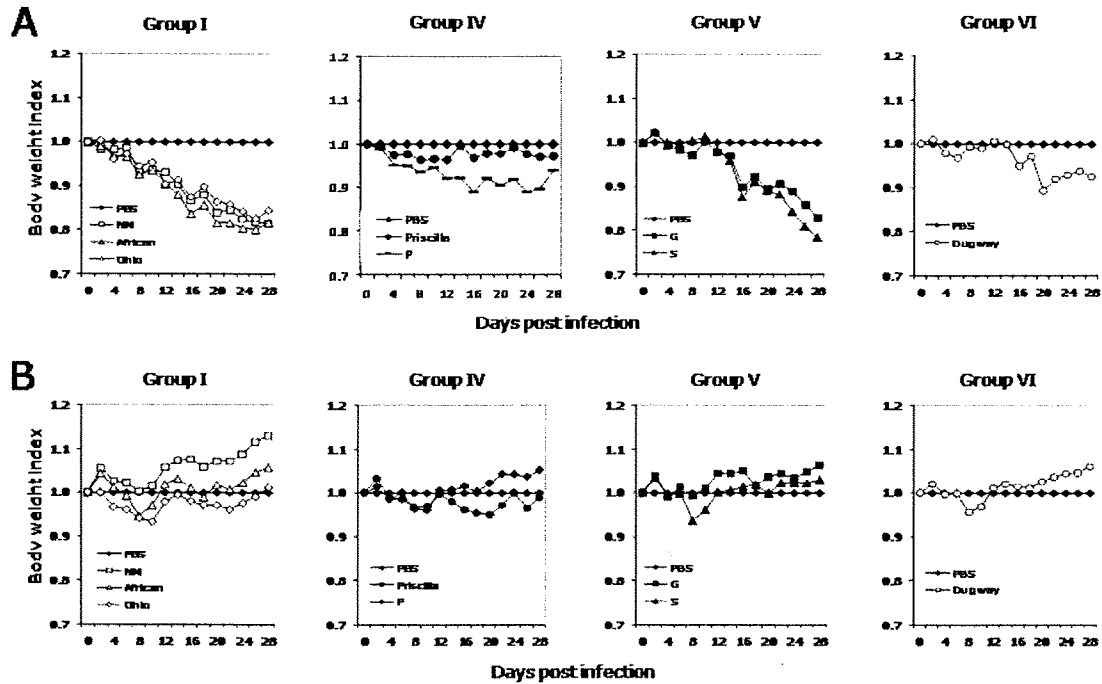


FIG. 1. Average body weight changes in SCID mice (A) and CB-17 mice (B) infected with *C. burnetii* isolates during 28 days of infection. Body weights were significantly lower in SCID mice throughout the infection period and transiently in CB-17 mice infected with all isolates except Priscilla compared to PBS-injected controls ($P < 0.05$).

late resulted in slow, progressive, and long-term-persistent disease. Clinical signs included ruffled fur, extremely distended abdomens, and death. Body weight loss, inactivity, and cachexia were not observed until a few days prior to death. Survival time ranged from 55 to 109 days p.i. Progression of clinical signs and survival times were dose dependent, with shorter times corresponding to higher infectious doses (see Table S2 in the supplemental material). Similar lesions were found in all of the SCID mice that died, most notably severe hepatosplenomegaly, and all organs had cellular infiltration, primarily macrophages containing bacteria. The severity of the lesions in infected SCID mice was not dependent on the *C. burnetii* challenge dose.

On the other hand, CB-17 and A/J mice displayed transitory clinical signs only after infection with the highest dose of Priscilla. Both mouse strains showed ruffled fur from 4 to 13 days p.i., but only A/J mice demonstrated transient body weight loss (data not shown). No other clinical signs were observed. At 28 days p.i., CB-17 and A/J mice had mild splenomegaly and seroconversion as evidence of infection (data not shown). Small granulomas were present in the spleen and liver, but bacterial antigen was not detectable by immunohistochemistry.

Genomic-group-specific virulence in mice. It was important to establish whether the results of infection seen with the Priscilla isolate and those previously noted with the NM isolate were genomic group specific (24). To determine this, the pathogenicities of multiple isolates were compared by delivering a single dose of eight *C. burnetii* isolates from four genomic groups (Table 1) to mice by i.p. injection. The infections were

initially compared in SCID and CB-17 mice sacrificed at 28 days p.i.

All *C. burnetii* isolates caused disease in SCID mice, with various clinical courses. There was no mortality during the 28-day infection period. Clinical signs, including significant body weight loss ($P < 0.05$) and cachexia, summarized in Fig. 1A and in Fig. S1A in the supplemental material, were most apparent in mice infected with group I isolates, followed by those given group V, IV, and VI isolates. In CB-17 mice, only mild transient disease was noted, with minimal loss of body weight, in response to all isolates and noticeably ruffled fur with group I isolate infection (Fig. 1B).

Splenomegaly in response to infection was more severe in SCID than in CB-17 mice (Fig. 2A). The number of bacteria in the spleens was determined by qPCR (Fig. 2B), and consistently higher numbers of *com1* genes were detected in SCID than in CB-17 mice. SCID mice showed phylogenetic-group-characteristic spleen size and growth of bacteria. Splenomegaly was greatest in SCID mice with mild clinical disease infected with bacteria from groups IV and VI. However, the number of organisms in the spleen was greater in mice with severe clinical disease following infection with phylogenetic groups I and V. In CB-17 mice, splenic enlargement and numbers of bacteria increased with the severity of clinical disease. CB-17 mice displayed differences between infection with the *C. burnetii* isolates that caused acute disease (phylogenetic group I) and infection with the *C. burnetii* isolates that caused chronic disease (phylogenetic groups IV and V), but there was no difference between groups infected with isolates that caused chronic disease. All infected mice developed significant splenomegaly,

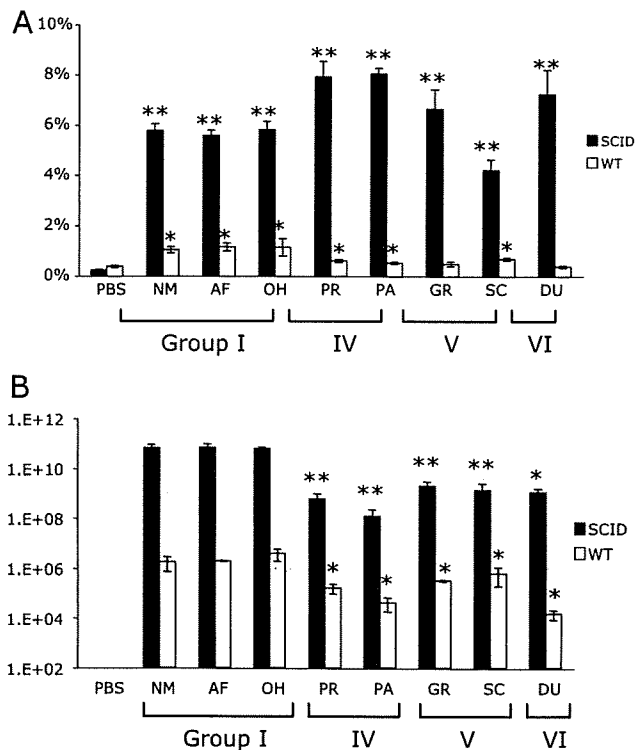


FIG. 2. Splenomegaly (A) and splenic bacterial loads (B) in mice at 28 days p.i. (A) All infected animals developed significant splenomegaly compared to controls, and infected SCID mice had significantly larger spleens than CB-17 mice ($P < 0.05$). (B) Mice infected with group IV, V, and VI isolates had significantly fewer bacteria than those infected with group I isolates ($P < 0.05$). *, $P < 0.05$. The error bars indicate standard deviations.

but mice infected with group IV, V, and VI isolates had significantly fewer splenic bacteria than mice infected with group I isolates ($P < 0.05$).

Evaluation of histopathology at 28 days p.i. revealed more lesions in SCID mice than in CB-17 mice (see Table S3 in the supplemental material). SCID mice showed histopathologic changes in all organs investigated. Group I isolates caused the most inflammation, followed by groups V, IV, and VI. The inflammatory-cell populations were similar in all groups and consisted of few neutrophils and numerous macrophages containing abundant intracytoplasmic bacteria. *C. burnetii* antigen was diffusely distributed in all organs examined. CB-17 mice had mild histopathologic changes in some organs, but even in the tissues with an inflammatory response, *C. burnetii* antigen was rarely detected.

Circulating cytokines are altered in *C. burnetii*-infected CB-17 mice. The variations in pathology and inflammation associated with these isolate group infections suggest differences in the immune responses. To expand on this observation, the serum levels of 16 cytokines and chemokines were measured. In CB-17 mice, serum cytokine levels differed between mice infected with group I isolates and those given isolates from other groups. Group I isolates induced persistently high cytokine secretion throughout the 28-day experiment; group IV and V isolates caused moderate cytokine secretion at the peak of clinical disease (7 to 14 days p.i.) (Fig. 3). After 14 days

p.i., group I isolates induced higher secretion of IL-3, IL-4, IL-6, IL-10, IL-12p40, IL-12p70, IFN- γ , TNF- α , MIP-1 α , and RANTES than other groups. The KC and granulocyte-macrophage colony-stimulating factor levels of mice infected with group I isolates were higher than those in mice infected with other groups prior to 14 days p.i. Serum IL-1 α , IL-1 β , IL-2, and IL-5 levels and eotaxin secretion were not increased during the infection period (data not shown).

Lethal potentials of all genomic groups in SCID mice. The lethal potentials of representative isolates from each phylogenetic group were investigated in SCID mice, and it was determined that all of the isolates evaluated could eventually lead to clinical illness and death in the immunodeficient model (see Fig. S1B in the supplemental material). Isolates that caused a long period of cachexia led to severe body weight loss in infected mice (see Fig. S2 in the supplemental material). A group I isolate (NM) induced the earliest and longest period of cachexia and, correspondingly, the most severe body weight loss. Mice infected with isolates from groups V (G) and VI (Dugway) had similar survival times, but those given group V isolates had longer periods of cachexia and more severe body weight loss than group VI-infected mice. Infection with group IV isolates (Priscilla and P) resulted in the shortest period of cachexia, and body weight loss was not observed until the terminal stage of infection. The survival time was shortest in mice challenged with group I isolates (32.0 ± 0.8 days), followed by those infected with groups V (36.0 ± 0.0 days), VI (35.5 ± 1.0 days), and IV (47.5 ± 0.6 days for P and 77.3 ± 2.8 days for Priscilla). The probable cause of death was multiple-organ failure due to massive systemic infection.

The pathological changes in SCID mice at mortality were more advanced than those observed at 28 days p.i. (data not shown). The severity of inflammatory changes in the liver and spleen was similar in all groups of infected mice, but animals given group I isolates exhibited a greater degree of inflammation in the heart and lungs than those given group IV, V, and VI isolates. The extent of splenomegaly changed with survival time; however, the numbers of bacteria in the spleen were similar in all groups, suggesting that the number of bacteria (10^{10} genome copies/spleen) detected is the saturation point in SCID mice. *C. burnetii* antigen was diffusely distributed in all tissue sections.

Genomic-group-specific outcome of acute Q fever pneumonia in the guinea pig aerosol model. Aerosol challenge in the guinea pig provides a physiologically relevant model that simulates both the natural route of infection and common clinical presentations associated with human acute Q fever, making this a choice model for evaluating the comparative levels of virulence of different *C. burnetii* isolates, and thus, it was used in the logical progression of experiments after different levels of virulence were observed in mouse models of infection. Guinea pigs challenged with group I and V isolates developed significant fever in response to infection ($P < 0.01$), whereas those given isolates from groups IV and VI were afebrile even at the highest challenge dose (Fig. 4).

Fever response, weight loss, and other clinical signs displayed a dose-dependent relationship in guinea pigs infected with the group I *C. burnetii* isolates African and Ohio, as has been described for the reference isolate in this group, NM (43). All animals that received African or Ohio organisms at a high

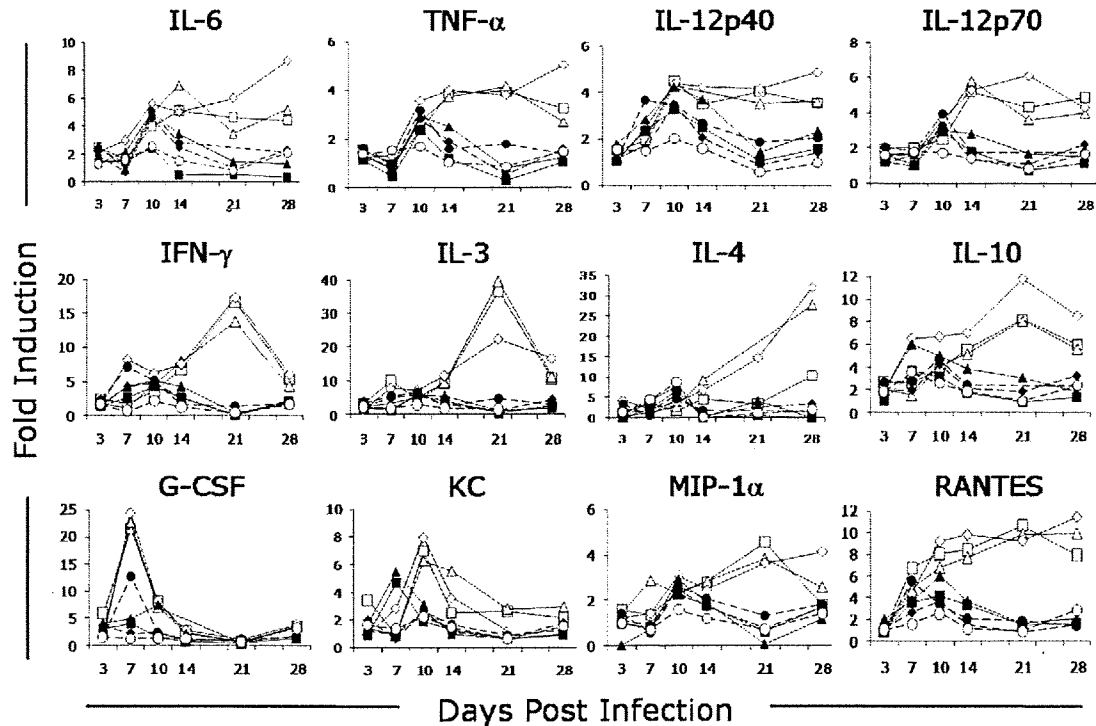


FIG. 3. Mean circulating cytokine levels in response to infection in CB-17 mice with different *C. burnetii* isolates. Isolates from genomic group I induced persistently high cytokine secretion with increased levels of IL-6, TNF- α , IL-12p40, IL-12p70, IFN- γ , IL-3, IL-4, IL-10, MIP-1 α , and RANTES compared with other genogroups ($P < 0.05$). \blacklozenge , PBS; \square , NM; \triangle , African; \diamond , Ohio; \bullet , Priscilla; \blacksquare , P; \blacktriangle , G; \circ , Dugway.

dose died within 7 to 9 days p.i., as did two of three that received NM; lower infectious doses were not lethal. Gross lung consolidation and overall lack of normal body fat were noted on necropsy at 7 to 9 days p.i. in guinea pigs infected with the highest dose of organisms. Histologically, these animals had severe panleukocytic bronchointerstitial pneumonia with bronchial and alveolar exudates. Lung tissues from the surviving NM-infected guinea pig and those given the mid-level dose of group I organisms were evaluated at 28 days p.i. for comparison to animals infected with other isolates evaluated at this time, and they exhibited moderate multifocal lymphohistiocytic pneumonia with granuloma formation.

No significant fever or other overt clinical signs were noted in guinea pigs infected with group IV isolates. Mild lymphohistiocytic pneumonia was seen histologically at 28 days p.i. in animals given the highest dose of organisms.

Group V isolate-infected guinea pigs all developed fever when given the highest challenge dose, and dose-dependent temperature increases and other clinical signs were again noted, with no fever development, in those animals receiving the lowest dose of organism. Though auscultation confirmed respiratory compromise, none of the infections were lethal. At 28 days p.i., the lungs had mild to moderate lymphohistiocytic interstitial pneumonia and a few small granulomas.

No major clinical or pathological changes were noted in guinea pigs infected with the group VI isolate or in negative control animals. Table S4 in the supplemental material compares the severity of histopathologic changes in guinea pigs infected with high doses of *C. burnetii* isolates from each group

at 28 days p.i. Immunohistochemistry confirmed the presence of *C. burnetii* organisms, primarily in macrophages, in the lungs, livers, and spleens of infected animals.

Experimental guinea pigs in all dose groups for each isolate seroconverted by the time of euthanasia, with the exception of animals infected with high doses of NM, African, and Ohio necropsied at 1 week p.i. and low-dose Dugway-infected guinea pigs. The degree of seroconversion was dose dependent and varied among isolates (data not shown). No PBS-injected control animals seroconverted.

Genomic-group-specific severity of hepatitis and splenomegaly in guinea pigs. The doughnut granulomas common in human acute Q fever hepatitis (31) had not been previously described in animals experimentally infected with *C. burnetii* and were also not seen in the guinea pigs in this study. Mild hepatitis and severe hepatic lipidosis were noted at death 7 days p.i. in guinea pigs challenged with high doses of group I isolates, as had been previously reported for NM aerosol-infected guinea pigs (43). Tissue sections from the remaining NM-infected guinea pig and those infected with mid-level doses of the group I organisms were evaluated for comparison with animals infected with other isolates at 28 days p.i. and revealed vacuolization and degeneration of centrilobular hepatocytes, lymphocyte infiltration in periportal regions, and multiple small granulomas.

Group IV-infected guinea pigs also had periportal lymphocytic infiltration, as well as multiple granulomas of various sizes. The granulomas in Priscilla- and P-infected guinea pigs were more defined, with more histiocytic involvement than was

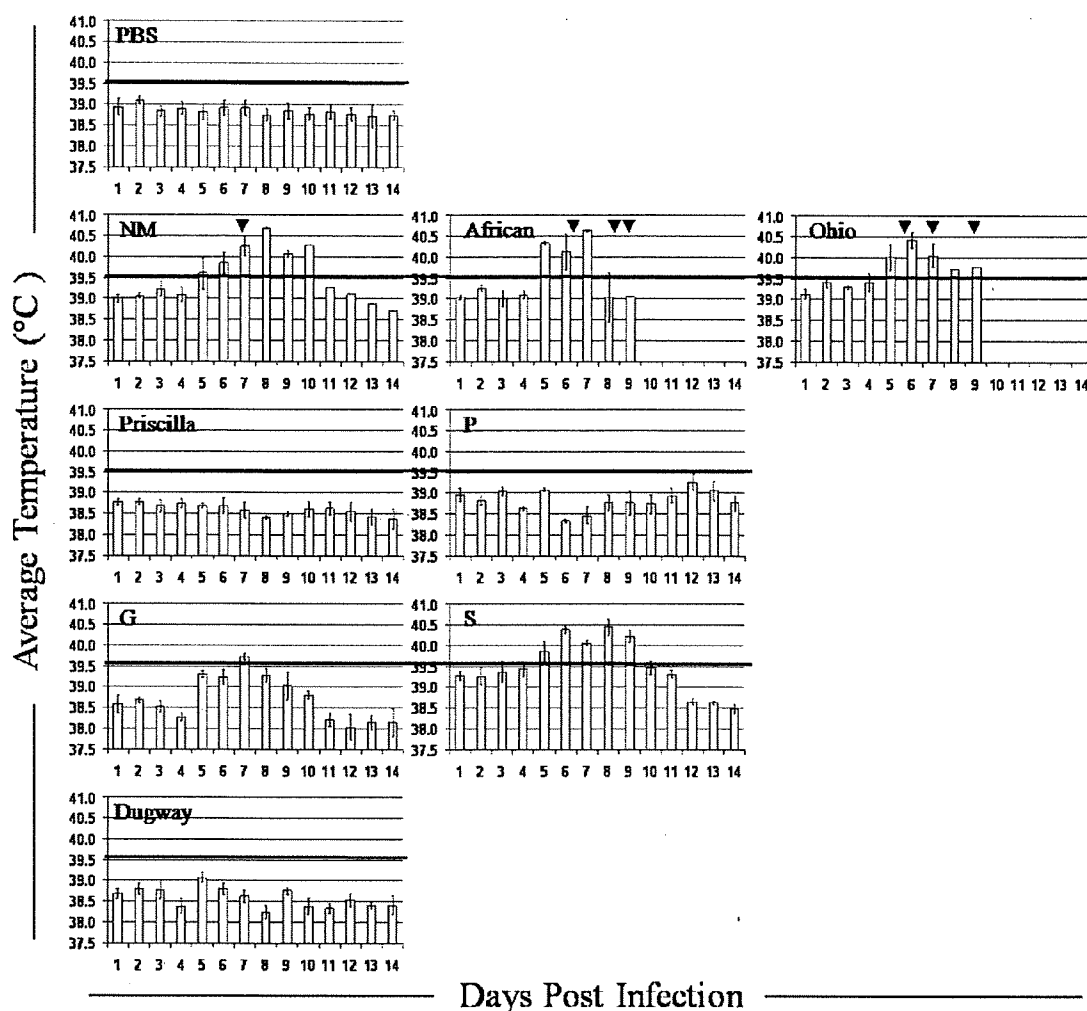


FIG. 4. Fever responses of guinea pigs to infection with high doses of *C. burnetii* isolates. The mean daily temperatures \pm standard errors of the mean ($n = 3$) of animals infected with 2×10^6 bacteria of each *C. burnetii* isolate. Temperatures of $\geq 39.5^\circ\text{C}$ (black lines) were considered fever. The arrows indicate days on which death occurred in NM-, African-, and Ohio-infected groups.

seen in guinea pigs infected with group I isolates. Subjectively, of all animals necropsied from each isolate group, hepatic granulomas from those infected with P were the greatest in size and number.

The livers of guinea pigs infected with the group V isolates G and S contained a few small granulomas and mild to moderate infiltration of lymphocytes along portal tracts. The hepatic changes observed in guinea pigs infected with group V isolates suggested that isolates from this group are less hepatovirulent than group IV isolates but more so than group I isolates.

No hepatic granulomas or other significant pathological changes were noted in guinea pigs infected with the group VI isolate Dugway. Liver weights did not vary significantly within or between genomic groups.

There were no significant differences in spleen weights at 28 days p.i. within or between genomic or dose groups. Animals infected with all isolates examined at 14 days p.i. (NM, P, G, and Dugway) had significantly larger spleens than PBS-in-

jected control animals, and spleens from NM- and G-infected guinea pigs were significantly larger ($P < 0.01$ and $P < 0.05$, respectively) than those of P- and Dugway-infected animals (see Fig. S3 in the supplemental material). Pathological findings included multiple small granulomas in the spleens of group I-infected guinea pigs; fewer small granulomas were occasionally noted in animals infected with group IV and V isolates.

Heterologous protection of cross-vaccination and challenge in guinea pigs. The infection studies described here illustrate that there is pathotype diversity between *C. burnetii* isolates from different genogroups, and they are consistent with phylogenetic studies cataloging distinct gene contents (4). We therefore strove to determine whether this diversity was great enough to affect the ability of vaccines to protect against infection. Guinea pigs were given group I (NM) or group IV (S) vaccine and cross-challenged to evaluate potential heterologous protection against high-dose infection. Nonvaccinated guinea pigs developed a noticeable fever response by day 5 p.i.,

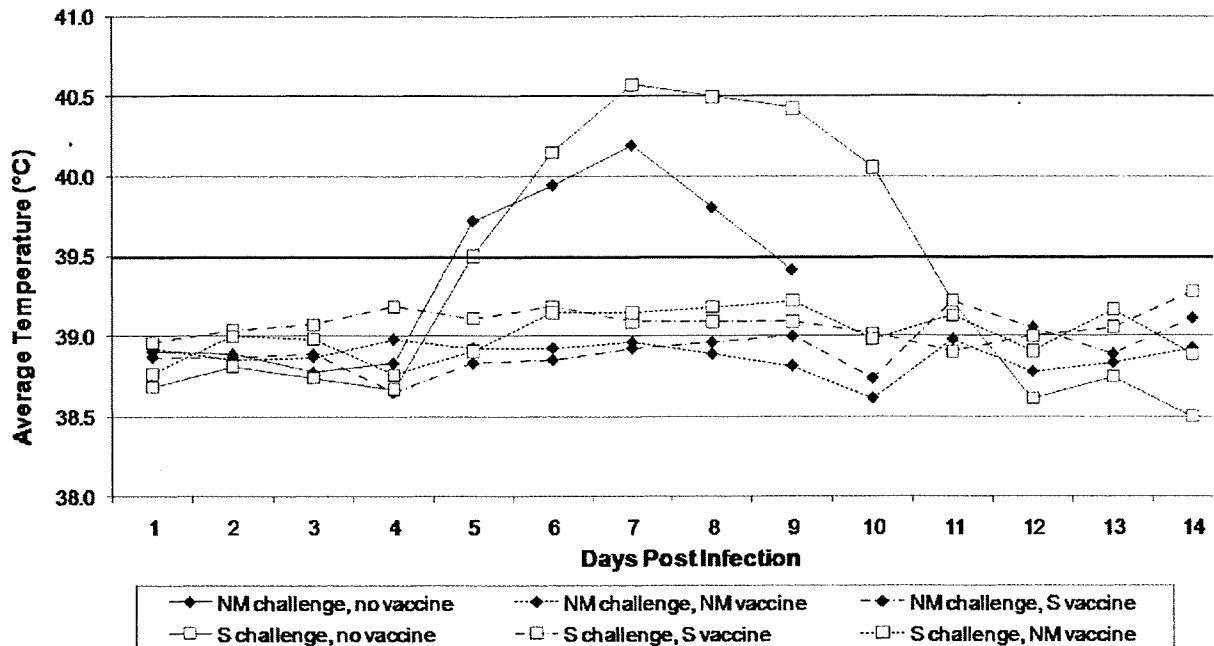


FIG. 5. Heterologous vaccination and challenge in guinea pigs. Shown are average daily temperatures of animals vaccinated with NM (dashed and dotted line), S (dashed line), or adjuvant alone (solid line) and challenged with high doses of NM (◆) or S (□). Temperatures of $\geq 39.5^{\circ}\text{C}$ were considered fever.

and infection was lethal in three of three NM- and one of three S-challenged animals. Guinea pigs vaccinated with either formalin-killed NM or S were completely protected against fever development and death when challenged with either NM or S (Fig. 5).

DISCUSSION

The potential for genomic-group-specific pathogenicity of *C. burnetii* was evaluated using immunocompetent mice and guinea pigs and immunodeficient mice. The hypotheses that isolates belonging to the same genomic group would cause similar disease and that there would be distinctions in disease manifestations between isolate groups were supported by the findings presented here.

A detailed analysis of the Priscilla isolate dose-effect in SCID mice revealed differences in virulence of *C. burnetii* isolates. Disease development after Priscilla infection was progressive but slower than the development of the disease caused by NM previously reported in SCID mice (1); the survival time of SCID mice infected with Priscilla was longer with the same LD_{50} . This result supports the previous study by Moos and Hackstadt that evaluated the lesser ability of the Priscilla isolate to cause fever in i.p.-challenged guinea pigs (36). Interestingly, the mice infected with Priscilla did not exhibit cachexia until the terminal stages of infection, when they had extremely severe hepatosplenomegaly. Although the disease caused by Priscilla was milder than that associated with NM, all mice that developed clinical illness died. This result confirms the high infectivity and lethal potential of *C. burnetii*, which is not restricted to isolates that cause acute disease, and suggests that

the SCID mouse model can be useful for evaluation of *C. burnetii* virulence.

The virulence of *C. burnetii* isolates tested in SCID mice was determined to be genomic group specific. Acute-Q fever-associated group I isolates caused the most rapidly progressing disease and the most severe pathological changes. Groups IV and V, isolates associated with chronic Q fever, caused a slower progression of disease. Overall, pathological changes in mice infected with group IV and V isolates were milder than those of group I-infected mice. The number of bacteria in the spleen at 28 days p.i. was greater in mice with severe disease from infection with group I isolates; however, the bacterial loads at the time of death were similar in all infected mice. This suggests that the rate of proliferation of *C. burnetii* in vivo may be virulence related. An in vitro comparison of infection in L929 cells using NM, Priscilla, and S isolates showed that all of the isolates could persistently infect, but Priscilla required a greater period of time to establish an infection (42), and it has been shown that inclusion-forming units produced by NM and Priscilla isolates were similar in Vero cells (36). However, because of developmental differences in clinical signs and pathological changes, the replication rate does not seem to be the only virulence factor involved, since clinical signs would then be similar with differences only in disease progression. At both time points, 28 days p.i. and the time of death due to infection, heart and lung lesions caused by group IV, V, and VI isolates were milder than those produced by infection with group I isolates. This observation seems to conflict with the hypothesis that isolates from chronic disease cause chronic Q fever, including heart disease. However, our observation is consistent with the report that isolates from heart lesions of

chronic-Q fever patients have genetic characteristics similar to those of isolates from acute disease (46). The hypothesis that isolates from acute disease do not cause endocarditis has been supported by two other research groups (17, 24). The correlation between virulence and phylogeny has been controversial because of a lack of comprehensive studies. One study detected genes specific to isolates from acute disease in isolates from chronic Q fever patients and concluded that the isolates were not disease specific (46). The isolates used in the study were isolated by cell culture, and although the cell culture system is highly effective for isolation, isolates from acute disease are known to infect cultured cells more efficiently than isolates from chronic disease, so there remains a potential that the study collected only cell culture-adapted isolates. Several *in vivo* studies have reported isolate-specific virulence using guinea pig and mouse models (17, 24, 36); however, the number of isolates used in these studies was limited, making it difficult to conclude that there was genomic-group-specific virulence. The present study using eight isolates from four phylogenetic groups strongly supports the variation in virulence among *C. burnetii* isolate groups.

In the absence of functional T and B cells, cytokine profiles showed no group-specific differences. In immunocompetent mice, group I isolates caused a stronger immune response with high levels of multiple cytokines over a longer time than other groups. Interestingly, Dugway (group VI) induced the least change in CB-17 mice. The inflammatory-cytokine changes in immunocompetent mice in this study were similar to those in humans with acute Q fever (10): TNF- α and IL-6 were upregulated, but IL-1 β was not. IFN- γ increased in CB-17 mice infected with group I isolates, and it is associated with the control of bacterial growth, stimulates phagosome-lysosome fusion, and may enable monocytes/macrophages to kill *C. burnetii* (13, 14). A difference in vacuole formation between isolates has also been shown, with NM and S developing within single large vacuoles while Priscilla occupied several smaller vacuoles per cell (18). This *in vitro* study suggested a difference in isolate ecology within host cells, which may be correlated with their virulence *in vivo*.

The ability to cause fever and respiratory illness was isolate and dose dependent in the guinea pig aerosol challenge model, with isolates from groups I and V causing disease consistent with human acute Q fever. Isolates within the same genomic group produced similar clinical illnesses, strongly supporting the mouse experiments demonstrating that genomic differences in the bacterial isolates do play a role in virulence. It was shown here that isolates associated with chronic disease, G and S, have the ability to cause acute disease in the guinea pig model. Our study confirmed and expanded the observations of Kazar et al. that the virulence of NM and S isolates was greater than that of Priscilla.

Lesny et al. compared the cross-immunity of whole-cell and soluble Q fever vaccines made from phase I NM, S, Priscilla, and Luga isolates. They found that vaccines from NM and Priscilla afforded a higher degree of protection than S and Luga vaccines and that whole-cell vaccines were more effective than soluble vaccines (28). In the guinea pig challenge study presented here, killed whole-cell vaccines made from isolates differing in LPS banding pattern (16), plasmid type (44), and genomic group (20), specifically isolates from groups I and V,

conferred heterologous protection against virulent high-dose challenge in accordance with previous studies (28). This suggests that although the manifestations of disease and genomic contents differ among various isolate groups, the antigenic properties of whole-cell vaccines are shared enough that cross-protection is possible. Such information is valuable for the design of new vaccines and could be of the utmost importance in offering reliable protection in the event of an outbreak.

The differences in perceived infectious doses noted when ODs, particle counts, and genome copy enumerations were compared underline the importance of using multiple quantitation methods to compare studies with earlier observations. Some of the differences in disease manifestations seen in guinea pigs in this study could be due to slight differences in the infectious doses delivered. For instance, Priscilla and P both induced hepatic changes, although guinea pigs infected with P appeared to develop more severe lesions than those infected with Priscilla, which had a lower infectious dose by OD and qPCR. The difference in infectious dose as determined by the genome copy number could account for this variation. However, G and S both caused fever, and although guinea pigs infected with G did not attain the same degree of febrile response as S-infected animals, quantitation by particle count and real-time PCR showed infectious doses of S to be over a log unit lower than those of G. It could be argued that Priscilla-infected guinea pigs did not develop fever because fewer bacteria were present in the aerosol challenge; however, the group IV isolates did not induce fever at any of the challenge doses while group I isolates induced fever even at the lowest dose. We believe that, despite the variation in the infectious dose depending on the enumeration technique, the significant differences noted among genotypic groups are valid.

Phase variation is the only well-characterized phenotypic difference that is related to virulence in *C. burnetii* (50). Although LPS may be a major virulence determinant, and isolate LPS banding patterns have been correlated with acute or chronic disease (16), other components alone or in association with LPS may be responsible for differences in mortality in SCID mice and fever development in aerosol-challenged guinea pigs. It has been hypothesized that differences in the lipid A component are responsible for the variations in virulence, but lipid structural information indicates they are similar. The combination of a variety of factors expressed by phase I bacteria likely governs the ability of *C. burnetii* to infect cells and to maintain continuous growth within the phagolysosome. Indeed, the combination of pathotype variation of disease in infected guinea pigs and cross-protection of different isolates suggests conserved predominant antigenic components with virulence determinant specificity.

A recent report compared all open reading frames of NM phase I to those of African, Ohio, P, G, S, and Dugway, among others (4), and a majority of the open reading frames deleted from NM in the other isolates were either hypothetical or nonfunctional; however, a few were associated with assorted cellular functions. Beare et al. compared the complete genome sequences of NM, K, G, and Dugway and found distinct collections of pseudogenes and unique gene contents that may contribute to pathotype-specific virulence, including type II and type IV secreted effector molecules (5). Integrating our *in vivo* data with these molecular details, as well as with other in

vitro studies, may reveal the critical virulence determinants of *C. burnetii* and ultimately identify targets for vaccine and therapeutic intervention.

Isolates of phase I *C. burnetii* have the potential to cause a range of clinical signs, including fever, pneumonia, hepatitis, and splenomegaly. Isolates from one human chronic-disease group induced mild to moderate acute disease in the physiologically relevant guinea pig aerosol challenge model, while a separate isolate group representing several chronic-disease isolates caused no acute disease. All isolates examined were capable of producing disease in the immunocompromised SCID mouse model, and genogroup-consistent trends were noted in cytokine production in response to infection in the immunocompetent-mouse model. In these studies, isolates within the same genomic group caused similar pathological responses, with a distinction in strain virulence between established genogroups, sustaining the theory that genetic differences in the bacterial isolates affect their virulence.

ACKNOWLEDGMENTS

This work was supported by funding from NIH NIAID grants KO8 AI055664, U54 AI057156, and RO1 AI057768 and Science Research Grant number 13460142 from the Ministry of Education, Science, Sports and Culture of Japan.

We are grateful to Laura R. Hendrix for critical review of the manuscript.

REFERENCES

- Andoh, M., T. Naganawa, A. Hotta, T. Yamaguchi, H. Fukushi, T. Masegi, and K. Hirai. 2003. SCID mouse model for lethal Q fever. *Infect. Immun.* 71:4717-4723.
- Arricau-Bouvery, N., Y. Hauck, A. Bejaoui, D. Frangoulidis, C. C. Bodier, A. Souriau, H. Meyer, H. Neubauer, A. Rodolakis, and G. Vergnaud. 2006. Molecular characterization of *Coxiella burnetii* isolates by infrequent restriction site-PCR and MLVA typing. *BMC Microbiol.* 6:38.
- Baumgartner, W., H. Dettlinger, N. Schmeer, and E. Hoffmeister. 1988. Evaluation of different fixatives and treatments for immunohistochemical demonstration of *Coxiella burnetii* in paraffin-embedded tissues. *J. Clin. Microbiol.* 26:2044-2047.
- Beare, P. A., J. E. Samuel, D. Howe, K. Virtaneva, S. F. Porcella, and R. A. Heinzen. 2006. Genetic diversity of the Q fever agent, *Coxiella burnetii*, assessed by microarray-based whole-genome comparisons. *J. Bacteriol.* 188:2309-2324.
- Beare, P. A., N. Unsworth, M. Andoh, D. E. Voth, A. Omsland, S. D. Gilk, K. P. Williams, B. W. Sobral, J. J. Kupko III, S. F. Porcella, J. E. Samuel, and R. A. Heinzen. 2008. Comparative genomics reveal extensive transposon-mediated genomic plasticity and diversity among potential effector proteins within the genus *Coxiella*. *Infect. Immun.* 77:642-656.
- Benenson, A. S., and W. D. Tigert. 1956. Studies on Q fever in man. *Trans. Assoc. Am. Physicians* 69:98-104.
- Benoit, M., E. Ghigo, C. Capo, D. Raoult, and J. L. Mege. 2008. The uptake of apoptotic cells drives *Coxiella burnetii* replication and macrophage polarization: a model for Q fever endocarditis. *PLoS Pathog.* 4:e1000066.
- Brennan, R. E., and J. E. Samuel. 2003. Evaluation of *Coxiella burnetii* antibiotic susceptibilities by real-time PCR assay. *J. Clin. Microbiol.* 41:1869-1874.
- Brouqui, P. 1993. Chronic Q fever. *Arch. Intern. Med.* 153:642-648.
- Capo, C., N. Amirayan, E. Ghigo, D. Raoult, and J. Mege. 1999. Circulating cytokine balance and activation markers of leucocytes in Q fever. *Clin. Exp. Immunol.* 115:120-123.
- Capo, C., Y. Zaffran, F. Zupan, P. Houpiquin, D. Raoult, and J. L. Mege. 1996. Production of interleukin-10 and transforming growth factor β by peripheral blood mononuclear cells in Q fever endocarditis. *Infect. Immun.* 64:4143-4150.
- Ghigo, E., C. Capo, D. Raoult, and J. L. Mege. 2001. Interleukin-10 stimulates *Coxiella burnetii* replication in human monocytes through tumor necrosis factor down-modulation: role in microbicidal defect of Q fever. *Infect. Immun.* 69:2345-2352.
- Ghigo, E., C. Capo, C. H. Tung, D. Raoult, J. P. Gorvel, and J. L. Mege. 2002. *Coxiella burnetii* survival in THP-1 monocytes involves the impairment of phagosome maturation: IFN- γ mediates its restoration and bacterial killing. *J. Immunol.* 169:4488-4495.
- Ghigo, E., A. Honstetter, C. Capo, J. P. Gorvel, D. Raoult, and J. L. Mege. 2004. Link between impaired maturation of phagosomes and defective *Coxiella burnetii* killing in patients with chronic Q fever. *J. Infect. Dis.* 190:1767-1772.
- Glazunova, O., V. Roux, O. Freylikman, Z. Sekeyova, G. Fournous, J. Tyczka, N. Tokarevich, E. Kovacava, T. J. Marrie, and D. Raoult. 2005. *Coxiella burnetii* genotyping. *Emerg. Infect. Dis.* 11:1211-1217.
- Hackstadt, T. 1986. Antigenic variation in the phase I lipopolysaccharide of *Coxiella burnetii* isolates. *Infect. Immun.* 52:337-340.
- Hackstadt, T. 1990. The role of lipopolysaccharides in the virulence of *Coxiella burnetii*. *Ann. N. Y. Acad. Sci.* 590:27-32.
- Hechemy, K. E., M. McKee, M. Marko, W. A. Samsonoff, M. Roman, and O. Baca. 1993. Three-dimensional reconstruction of *Coxiella burnetii*-infected L929 cells by high-voltage electron microscopy. *Infect. Immun.* 61:4485-4488.
- Hendrix, L., and L. P. Mallavia. 1984. Active transport of proline by *Coxiella burnetii*. *J. Gen. Microbiol.* 130:2857-2863.
- Hendrix, L. R., J. E. Samuel, and L. P. Mallavia. 1991. Differentiation of *Coxiella burnetii* isolates by analysis of restriction-endonuclease-digested DNA separated by SDS-PAGE. *J. Gen. Microbiol.* 137:269-276.
- Honstetter, A., G. Imbert, E. Ghigo, F. Gouriet, C. Capo, D. Raoult, and J. L. Mege. 2003. Dysregulation of cytokines in acute Q fever: role of interleukin-10 and tumor necrosis factor in chronic evolution of Q fever. *J. Infect. Dis.* 187:956-962.
- Huebner, R. J., W. L. Jellison, and M. D. Beck. 1949. Q fever studies in southern California. III. Effects of pasteurization on survival of *Coxiella burnetii* in naturally infected milk. *Public Health Rep.* 64:499-511.
- Jager, C., H. Willems, D. Thiele, and G. Baljer. 1998. Molecular characterization of *Coxiella burnetii* isolates. *Epidemiol. Infect.* 120:157-164.
- Kazar, J., M. Lesny, P. Propper, D. Valkova, and R. Brezina. 1993. Comparison of virulence for guinea pigs and mice of different *Coxiella burnetii* phase I strains. *Acta Virol.* 37:437-448.
- Koster, F. T., J. C. Williams, and J. S. Goodwin. 1985. Cellular immunity in Q fever: modulation of responsiveness by a suppressor T cell-monocyte circuit. *J. Immunol.* 135:1067-1072.
- La Scola, B., H. Lepidi, and D. Raoult. 1997. Pathologic changes during acute Q fever: influence of the route of infection and inoculum size in infected guinea pigs. *Infect. Immun.* 65:2443-2447.
- Lennette, E. H., W. H. Clark, M. M. Abinanti, O. Brunetti, and J. M. Covert. 1952. Q fever studies. XIII. The effect of pasteurization on *Coxiella burnetii* in naturally infected milk. *Am. J. Hyg.* 55:246-253.
- Lesny, M., J. Kazar, P. Propper, and M. Lukacova. 1991. Virulence and cross-immunity study on guinea pigs infected with different phase I *Coxiella burnetii* strains, p. 666-673. In J. Kazar and D. Raoult (ed.), *Rickettsiae and rickettsial diseases*. Publishing House of the Slovak Academy of Sciences, Bratislava, Slovakia.
- Madariaga, M. G., J. Pulvirenti, M. Sekosan, C. D. Paddock, and S. R. Zaki. 2004. Q fever endocarditis in HIV-infected patients. *Emerg. Infect. Dis.* 10:501-504.
- Marrie, T. J. 1990. Acute Q fever, p. 125-160. In T. J. Marrie (ed.), *Q fever*, vol. 1. The disease. CRC Press, Boca Raton, FL.
- Marrie, T. J. 1990. Q fever hepatitis, p. 171-178. In T. J. Marrie (ed.), *Q fever*, vol. 1. The disease. CRC Press, Boca Raton, FL.
- Marrie, T. J. 2004. Q fever pneumonia. *Curr. Opin. Infect. Dis.* 17:137-142.
- Marrie, T. J., A. Stein, D. Janigan, and D. Raoult. 1996. Route of infection determines the clinical manifestations of acute Q fever. *J. Infect. Dis.* 173:484-487.
- Maurin, M., and D. Raoult. 1999. Q fever. *Clin. Microbiol. Rev.* 12:518-553.
- McMurray, D. N. 1994. Guinea pig model of tuberculosis, p. 135-147. In B. R. Bloom (ed.), *Tuberculosis: pathogenesis, protection, and control*. American Society for Microbiology, Washington, DC.
- Moos, A., and T. Hackstadt. 1987. Comparative virulence of intra- and interstrain lipopolysaccharide variants of *Coxiella burnetii* in the guinea pig model. *Infect. Immun.* 55:1144-1150.
- Ormsbee, R. A. 1965. Q fever rickettsia, p. 1144-1160. In F. L. Horsfall and I. Tamm (ed.), *Viral and rickettsial diseases of man*. J. B. Lippincott, Philadelphia, PA.
- Reference deleted.
- Penttila, I. A., R. J. Harris, P. Storm, D. Haynes, D. A. Worswick, and B. P. Marmion. 1998. Cytokine dysregulation in the post-Q-fever fatigue syndrome. *QJM* 91:549-560.
- Raoult, D., and T. Marrie. 1995. Q Fever. *Clin. Infect. Dis.* 20:489-496.
- Raoult, D., A. Raza, and T. J. Marrie. 1990. Q fever endocarditis and other forms of chronic Q fever, p. 179-120. In T. J. Marrie (ed.), *Q fever*, vol. 1. The disease. CRC Press, Boca Raton, FL.
- Roman, M. J., H. A. Crissman, W. A. Samsonoff, K. E. Hechemy, and O. G. Baca. 1991. Analysis of *Coxiella burnetii* isolates in cell culture and the expression of parasite-specific antigens on the host membrane surface. *Acta Virol.* 35:503-510.
- Russell-Lodrigue, K. E., G. Q. Zhang, D. N. McMurray, and J. E. Samuel. 2006. Clinical and pathologic changes in a guinea pig aerosol challenge model of acute Q fever. *Infect. Immun.* 74:6085-6091.
- Samuel, J. E., M. E. Frazier, and L. P. Mallavia. 1985. Correlation of

- plasmid type and disease caused by *Coxiella burnetii*. *Infect. Immun.* **49**:775-779.
45. Scott, G. H., J. C. Williams, and E. H. Stephenson. 1987. Animal models in Q fever: pathological responses of inbred mice to phase I *Coxiella burnetii*. *J. Gen. Microbiol.* **133**:691-700.
 46. Stein, A., and D. Raoult. 1993. Lack of pathotype specific gene in human *Coxiella burnetii* isolates. *Microb. Pathog.* **15**:177-185.
 47. Stoenner, H. G., R. Holdenried, D. Lackman, and J. S. Orsborn. 1959. The occurrence of *Coxiella burnetii*, *Brucella*, and other pathogens among fauna of the Great Salt Lake Desert in Utah. *Am. J. Trop. Med. Hyg.* **8**:590-595.
 48. Stoenner, H. G., and D. B. Lackman. 1960. The biologic properties of *Coxiella burnetii* isolated from rodents collected in Utah. *Am. J. Hyg.* **71**:45-51.
 49. Svraha, S., R. Toman, L. Skultety, K. Slaba, and W. L. Homan. 2006. Establishment of a genotyping scheme for *Coxiella burnetii*. *FEMS Microbiol. Lett.* **254**:268-274.
 50. Thiele, D., and H. Willems. 1994. Is plasmid based differentiation of *Coxiella burnetii* in 'acute' and 'chronic' isolates still valid? *Eur. J. Epidemiol.* **10**:427-434.
 51. Tissot Dupont, H., D. Raoult, P. Brouqui, F. Janbon, D. Peyramond, P. J. Weiller, C. Chicheportiche, M. Nezri, and R. Poirier. 1992. Epidemiologic features and clinical presentation of acute Q fever in hospitalized patients: 323 French cases. *Am. J. Med.* **93**:427-434.
 52. Wiegshauss, E. H., D. N. McMurray, A. A. Grover, G. E. Harding, and D. W. Smith. 1970. Host-parasite relationships in experimental airborne tuberculosis. 3. Relevance of microbial enumeration to acquired resistance in guinea pigs. *Am. Rev. Respir. Dis.* **102**:422-429.
 53. Williams, J. C., M. G. Peacock, and T. F. McCaul. 1981. Immunological and biological characterization of *Coxiella burnetii*, phase I and phase II, separated from host components. *Infect. Immun.* **32**:840-851.
 54. Zhang, G. Q., and J. E. Samuel. 2003. Identification and cloning potentially protective antigens of *Coxiella burnetii* using sera from mice experimentally infected with Nine Mile phase I. *Ann. N. Y. Acad. Sci.* **990**: 510-520.

Editor: R. P. Morrison

Evolutional and Geographical Relationships of *Bartonella grahamii* Isolates from Wild Rodents by Multi-locus Sequencing Analysis

Kai Inoue · Hidenori Kabeya · Michael Y. Kosoy ·
Ying Bai · George Smirnov · Dorothy McColl ·
Harvey Artsob · Soichi Maruyama

Received: 22 June 2008 / Accepted: 19 January 2009 / Published online: 14 February 2009
© Springer Science + Business Media, LLC 2009

Abstract To clarify the relationship between *Bartonella grahamii* strains and both the rodent host species and the geographic location of the rodent habitat, we have investigated 31 *B. grahamii* strains from ten rodent host species from Asia (Japan and China), North America (Canada and the USA), and Europe (Russia and the UK). On the basis of multi-locus sequencing analysis of 16S rRNA, *ftsZ*, *gltA*, *groEL*, *ribC*, and *rpoB*, the strains were classified into two large groups, an Asian group and an American/European group. In addition, the strains examined were clearly clustered according to the geographic locations where the rodents had been captured. In the phylogenetic analysis based on *gltA*, the Japanese strains were divided into two subgroups: one close to strains from China, and the other

related to strains from Far Eastern Russia. Thus, these observations suggest that the *B. grahamii* strains distributed in Japanese rodents originated from two different geographic regions. In the American/European group, *B. grahamii* from the North American continent showed an ancestral lineage and strict host specificity; by contrast, European strains showed low host specificity. The phylogenetic analysis and host specificity of *B. grahamii* raise the possibility that *B. grahamii* strains originating in the North American continent were distributed to European countries by adapting to various rodent hosts.

Introduction

The genus *Bartonella* was formerly classified as the genera *Bartonella*, *Grahamella*, and *Rochalimaea*. These microorganisms are Gram-negative, fastidious, and hemotropic bacteria that are mainly transmitted by blood-sucking arthropod vectors [7]. The genus *Bartonella* now consists of 20 species and three subspecies; 11 species or subspecies of them, including *Bartonella birtlesii* [2], *Bartonella dohiae* [4], *Bartonella elizabethae* [8], *Bartonella grahamii* [4], *Bartonella phoceensis* [12], *Bartonella rattimassiliensis* [12], *Bartonella taylorii* [4], *Bartonella tribocorum* [14], *Bartonella vinsonii* subsp. *arupensis* [35], *Bartonella vinsonii* subsp. *vinsonii* [5, 22], and *Bartonella washoensis* [23] have been isolated from diverse wild rodent species. Some *Bartonella* species have been shown to have strict host specificity in epidemiological studies [6, 17, 24] and by experimental infection using cotton rats (*Sigmodon hispidus*), white-footed mice (*Peromyscus leucopus*), and other rodent species together with specific *Bartonella* species [25].

K. Inoue · H. Kabeya · S. Maruyama (✉)
Laboratory of Veterinary Public Health,
Department of Veterinary Medicine,
College of Bioresource Sciences, Nihon University,
1866 Kameino, Fujisawa,
Kanagawa 252-8510, Japan
e-mail: maruyama.soichi@nihon-u.ac.jp

M. Y. Kosoy · Y. Bai
Division of Vector-Borne Infectious Diseases,
National Center for Infectious Diseases,
Centers for Disease Control and Prevention,
Fort Collins, CO, USA

G. Smirnov
Gamaleya Research Institute of Epidemiology and Microbiology,
Russian Academy of Medical Sciences,
Moscow, Russia

D. McColl · H. Artsob
National Microbiology Laboratory,
Public Health Agency of Canada,
Winnipeg, MB, Canada

B. grahamii was first isolated from *Myodes glareolus* (formerly *Clethrionomys glareolus*) in the UK in 1995 [3]. Subsequently, it was shown that this bacterial species is widely distributed all over the world, including Asia [16, 29, 36], Europe [9, 15, 33], and North America [10, 17], and *B. grahamii* has been isolated from various rodent species—namely, the genera *Myodes*, *Apodemus*, *Microtus*, *Mus*, and *Dryomys*. In a clinical study, the DNA of *B. grahamii* was detected in the ocular fluid of a patient with neuroretinitis [20], suggesting that the organism is potentially pathogenic to human. Despite its widespread distribution, little is known about how *B. grahamii* strains from different countries in Asia, Europe, and North America are related.

In this study, we have investigated the relationship between *B. grahamii* strains and both the host rodent species and the geographic location of the host habitat by analyzing the DNA sequences of strains from rodents in Japan, China, Canada, the USA, Russia, and the UK. For this purpose, we performed multi-locus sequencing analysis (MLSA), targeting the genes encoding 16S rRNA [13], cell-division protein (*ftsZ*) [38], citrate synthase (*gltA*) [30], 60 kDa heat-shock protein (*groEL*) [37], riboflavin synthase alpha chain (*ribC*) [1, 18], and RNA polymerase beta subunit (*rpoB*) [31].

Materials and Methods

Bacterial Strains and Culture Conditions

A total of 31 *B. grahamii* strains, including the type strain, were used in this study (Table 1). These strains were isolated from ten rodent species: a large Japanese field mouse (*Apodemus speciosus*, $n=10$), a small Japanese field mouse (*Apodemus argenteus*, $n=5$), a Chevrier's field mouse (*Apodemus chevrieri*, $n=1$), a south China field mouse (*Apodemus draco*, $n=1$), a large-eared field mouse (*Apodemus latronum*, $n=2$), a Gapper's red-backed vole (*Myodes gapperi*, $n=6$), a prairie vole (*Microtus ochrogaster*, $n=3$), an Ural field mouse (*Apodemus uralensis*, $n=1$), a yellow-necked mouse (*Apodemus flavicollis*, $n=1$), and a bank vole (*Myodes glareolus*, $n=1$). The strains were derived from six countries: Japan ($n=15$), China ($n=4$), Canada ($n=6$), the USA ($n=3$), Russia ($n=2$), and the UK ($n=1$). All of these strains were genetically identified as *B. grahamii* by sequencing a fragment of *gltA* before the present study. In addition, the sequence information of *gltA* of *B. grahamii* obtained from a house mouse (*Mus musculus*) captured in California, USA (GenBank accession number AF086637) and those of *B. grahamii* from the spleen and liver of rodents (*Apodemus peninsulae* and *Apodemus agrarius*) in Far Eastern Russia (AY584854–AY584857) were also included in this study [10, 29].

All bacterial strains were cultured on heart infusion agar plates (DIFCO, MI, USA) containing 5% defibrinated rabbit blood. The plates were cultured at 35°C in a 5% CO₂ atmosphere for 2 weeks, and harvested bacteria were used for DNA extraction.

DNA Extraction and Polymerase Chain Reaction (PCR) of 16S rRNA, *ftsZ*, *gltA*, *groEL*, *ribC*, and *rpoB*

Genomic DNA was extracted from each strain by using an Instagene Matrix (Bio Rad, CA, USA). The extracted DNA was used for PCR amplification of 16S rRNA, *ftsZ*, *gltA*, *groEL*, *ribC*, and *rpoB* [27]. The PCR amplification of each gene was performed in a volume of 20 µl containing 20 ng of extracted DNA, 200 µM each of dATP, dGTP, dCTP, and dTTP, 1.5 mM MgCl₂, 0.5 U of *Taq* DNA polymerase (Promega, WI, USA), and 1 pmol of each primer. The primers and PCR conditions for 16S rRNA [13], *ftsZ* [38], *gltA* [30], *groEL* [37], and *rpoB* [31] were the same as described in previous reports. The primer pair for *ribC* was originally designed in this study as ribC5'-NU (5'-ARA-TGGAGGCGTAAGAYAYT-3') and ribC3'-NU (5'-AARC-GYGCTTCAACAATCAA-3'), and the PCR conditions for amplification of *ribC* were as follows: denaturation at 94°C for 4 min, 35 cycles of denaturation at 94°C for 30 s, annealing at 49°C for 30 s, extension at 72°C for 60 s, and a final extension at 72°C for 7 min.

Direct DNA Sequencing Analysis

The PCR products were purified by using a SpinColumn PCR Product Purification Kit (Bio Basic, Ontario, Canada). Direct DNA sequencing of the purified PCR products was carried out by dye terminator chemistry with specific primers for 16S rRNA [13], *ftsZ* [38], *gltA* [30], *groEL* [37], and *rpoB* [31] and for *ribC* (see above) using a Genetic Analyzer model 3130 (Applied Biosystem, CA, USA).

Phylogenetic Analysis and Construction of Phylogenetic Trees

The sequence data for 16S rRNA (1,348 bp), *ftsZ* (788 bp), *gltA* (312 bp), *groEL* (1,185 bp), *ribC* (618 bp), and *rpoB* (825 bp) from the 31 *B. grahamii* strains were aligned with those of the type strains of *Bartonella* species by using CLUSTAL X version 1.83 [34]. A phylogenetic tree covering 5,076 bp of concatenated data from the six loci was drawn by using the neighbor-joining (NJ) method [32] in the MEGA 3.1 software program [26] with the Jukes-Cantor parameters method [19], which is based on the assumption that all nucleotide substitutions are equally likely. Bootstrap analysis was carried out on 1,000 replications [11].

Table 1 Geographical origin, host rodent species, and GenBank accession numbers of the six loci used for MLSA of 31 *B. grahmanni* strains

No.	Country/location	Host rodent species	Strain	GenBank accession number					
				16S rRNA	<i>ftsZ</i>	<i>gltA</i>	<i>groEL</i>	<i>ribC</i>	<i>rpoB</i>
1	Japan/Hokkaido	<i>Apodemus speciosus</i>	Hokkaido 4-1	AB426629	AB426638	AB426652	AB426657	AB426678	AB426691
2	Japan/Hokkaido	<i>A. argentens</i>	Hokkaido 48-1	AB426630	AB426639	Identical to No. 1	Identical to No. 1	Identical to No. 1	AB426692
3	Japan/Aomori	<i>A. speciosus</i>	Aomori 23-1	Identical to No. 1	AB426640	Identical to No. 1	AB426658	Identical to No. 1	AB259947
4	Japan/Aomori	<i>A. argentens</i>	Aomori 40-1	Identical to No. 1	Identical to No. 3	Identical to No. 1	Identical to No. 1	Identical to No. 1	Identical to No. 1
5	Japan/Kanagawa	<i>A. speciosus</i>	Fujisawa 5-1	Identical to No. 1	Identical to No. 1	Identical to No. 1	AB426659	Identical to No. 1	Identical to No. 1
6	Japan/Kanagawa	<i>A. argentens</i>	Fujisawa 1-1	Identical to No. 1	Identical to No. 3	Identical to No. 1	Identical to No. 3	Identical to No. 1	Identical to No. 1
7	Japan/Shizuoka	<i>A. speciosus</i>	Fuji 4-1	Identical to No. 1	AB426641	Identical to No. 1	AB426660	Identical to No. 1	Identical to No. 1
8	Japan/Shizuoka	<i>A. argentens</i>	Fuji 6-1	Identical to No. 2	Identical to No. 2	Identical to No. 1	AB426661	Identical to No. 1	AB242285
9	Japan/Nagano	<i>A. speciosus</i>	Nagano 3-1	Identical to No. 1	Identical to No. 2	Identical to No. 1	AB426662	Identical to No. 1	AB290260
10	Japan/Nagano	<i>A. argentens</i>	Nagano 32-1	Identical to No. 1	Identical to No. 3	AB290289	Identical to No. 1	Identical to No. 1	Identical to No. 1
11	Japan/Ishikawa	<i>A. speciosus</i>	Ishikawa 4-1	Identical to No. 2	Identical to No. 3	Identical to No. 1	Identical to No. 1	Identical to No. 1	Identical to No. 1
12	Japan/Tokushima	<i>A. speciosus</i>	Tokushima 4-1	AB426631	AB426642	AB290291	AB426663	AB426679	AB426693
13	Japan/Ehime	<i>A. speciosus</i>	Ehime 1-1	Identical to No. 12	Identical to No. 12	AB426653	AB426664	Identical to No. 12	Identical to No. 12
14	Japan/Kagoshima	<i>A. speciosus</i>	Nakanoshima 7-1	Identical to No. 2	Identical to No. 1	Identical to No. 1	Identical to No. 8	AB426680	Identical to No. 1
15	Japan/Kagoshima	<i>A. speciosus</i>	Nakanoshima 10-1	Identical to No. 12	Identical to No. 12	Identical to No. 13	AB426665	Identical to No. 12	Identical to No. 12
16	China/Yunnan	<i>A. chevrieri</i>	Ac1692yn	AB426632	AB426643	AF391271	AB426666	AB426681	AB426694
17	China/Yunnan	<i>A. draco</i>	Ad1734yn	AB426633	AB426644	AF391277	AB426667	AB426682	AB426695
18	China/Yunnan	<i>A. latronum</i>	AL1707yn	Identical to No. 18	AB426645	AF391275	AB426668	AB426683	AB426696
19	China/Yunnan	<i>A. latronum</i>	AL1714yn	Identical to No. 18	Identical to No. 16	AF391280	AB426669	AB426684	AB426697
20	Russia/Moscow	<i>A. uralensis</i>	PT7B 29/18	AB426634	AB426646	Identical to No. 31	AB426675	AB426689	Identical to No. 31
21	Russia/Moscow	<i>A. flavicollis</i>	PTZA 30/3	Identical to No. 21	AB426647	Identical to No. 31	AB426676	Identical to No. 20	Identical to No. 31
22	Canada/Alberta	<i>Myodes gapperi</i>	Cg4224alb	Identical to No. 1	AB426648	AB426654	AB426670	AB426685	AB426698
23	Canada/Alberta	<i>M. gapperi</i>	Cg4226alb	Identical to No. 1	Identical to No. 22	Identical to No. 22	AB426671	AB426686	AB426699
24	Canada/Alberta	<i>M. gapperi</i>	Cg4227alb	Identical to No. 1	Identical to No. 22	Identical to No. 22	AB426672	Identical to No. 23	Identical to No. 23
25	Canada/Alberta	<i>M. gapperi</i>	Cg4228alb	Identical to No. 1	Identical to No. 22	Identical to No. 22	AB426673	AB426687	AB426700
26	Canada/Alberta	<i>M. gapperi</i>	Cg4263alb	AB426635	AB426649	Identical to No. 22	AB426674	AB426688	AB426701
27	Canada/Alberta	<i>M. gapperi</i>	Cg4285alb	AB426636	Identical to No. 26	Identical to No. 22	Identical to No. 26	Identical to No. 26	Identical to No. 26
28	USA/South Dakota	<i>Microtus ochrogaster</i>	B12509	Identical to No. 1	AB426650	AB426655	AB426677	AB426690	AB426702
29	USA/South Dakota	<i>Mi. ochrogaster</i>	B12511	AB426637	AB426651	AB426656	Identical to No. 28	Identical to No. 28	Identical to No. 28
30	USA/South Dakota	<i>Mi. ochrogaster</i>	B12512	Identical to No. 1	Identical to No. 29	Identical to No. 28	Identical to No. 28	Identical to No. 28	Identical to No. 28
31	UK/Shropshire	<i>M. glareolus</i>	V2 ^T	Z31349	AF467753	Z70016	AF014833	AY166583	AF165993

^T type strain

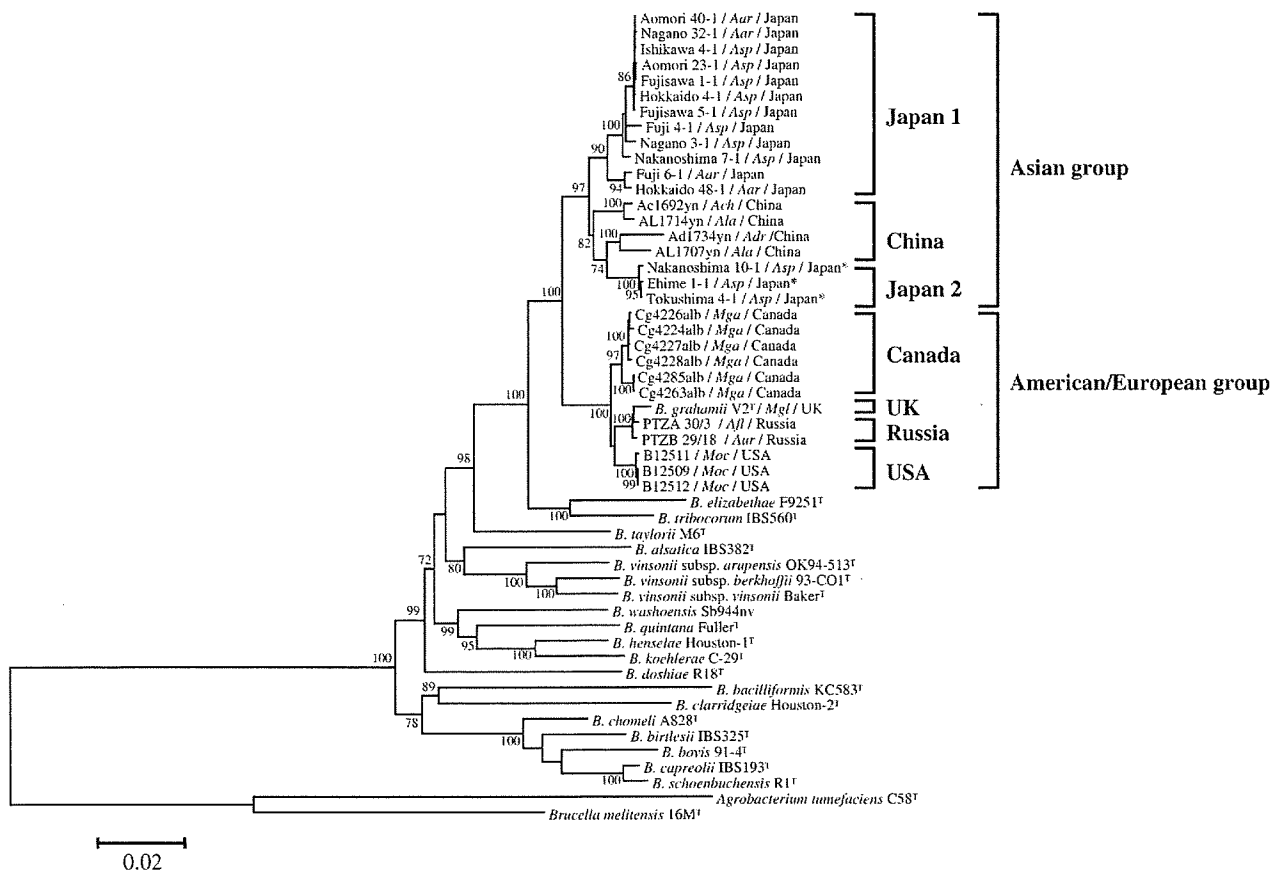


Figure 1 Phylogenetic tree of the 31 *B. grahamii* strains examined here and known *Bartonella* species constructed by the NJ method with Jukes–Cantor parameters based on the concatenated nucleotide sequences (5,076 bp) of 16 S rRNA, *ftsZ*, *gltA*, *groEL*, *ribC*, and *rpoB*. The derived host rodent species and the country of origin of the strains are shown after each slash. Bootstrap values (percentage of 1,000 replications) of >70% are indicated at the node. The sequences

of *Brucella melitensis* strain 16M and *Agrobacterium tumefaciens* strain C58 have been chosen as outgroups in the phylogenetic tree. The abbreviations of the host species are as follows: *Aar*, *Apodemus argenteus*; *Ach*, *Apodemus chevrieri*; *Adr*, *Apodemus draco*; *Afl*, *Apodemus flavicollis*; *Ala*, *Apodemus latronum*; *Asp*, *Apodemus speciosus*; *Aur*, *Apodemus uralensis*; *Mga*, *Myodes gapperi*; *Mgl*, *Myodes glareolus*; and *Moc*, *Microtus ochrogaster*

In addition to the *gltA* sequence from the 31 strains, five *gltA* sequences of strains from a *Mu. musculus* host captured in California, USA (AF086637), and from *A. peninsulae* and *A. agrarius* hosts in Far Eastern Russia (AY584854–AY584857) were also included in the following analysis. The data for the 36 *gltA* sequences were aligned with those of the type strains of *Bartonella* species by the same method used for the concatenated sequences of the six loci, and a phylogenetic tree based on *gltA* was constructed by the NJ method with Kimura’s two-parameter distance method [21].

Results

Phylogenetic Analysis by using the Concatenated Sequences of the Six Loci

The DNA fragments of all six loci, including 16S rRNA, *ftsZ*, *gltA*, *groEL*, *ribC*, and *rpoB*, of the 31 *B. grahamii* strains

were successfully sequenced and GenBank accession numbers were obtained (Table 1). The strains were classified into 10, 15, 12, 22, 14, and 16 sequence types (STs) for 16S rRNA, *ftsZ*, *gltA*, *groEL*, *ribC*, and *rpoB*, respectively. The sequence similarity of the concatenated sequences (5,076 bp) of the strains according to country was 97.8–100% in Japan, 97.3–99.6% in China, 99.5–100% in Canada, 99.9–100% in the USA, and 99.8% in Russia. The sequence similarity of the strains according to host rodent genera was 95.5–99.9% in *Apodemus* mice, 98.2–99.9% in *Myodes* voles, and 99.9–100% in *Microtus* voles.

The phylogenetic tree based on the concatenated sequences is shown in Fig. 1. The strains branched to two large groups, an Asian group and an America/European group, with a high bootstrap value (>97%). In the Asian group, *B. grahamii* strains derived from Japan were classified into two sub-groups, termed Japan 1 and Japan 2. Although the strains in Japan 1, which were derived from geographic locations throughout Japan, formed a separate clade, three strains in

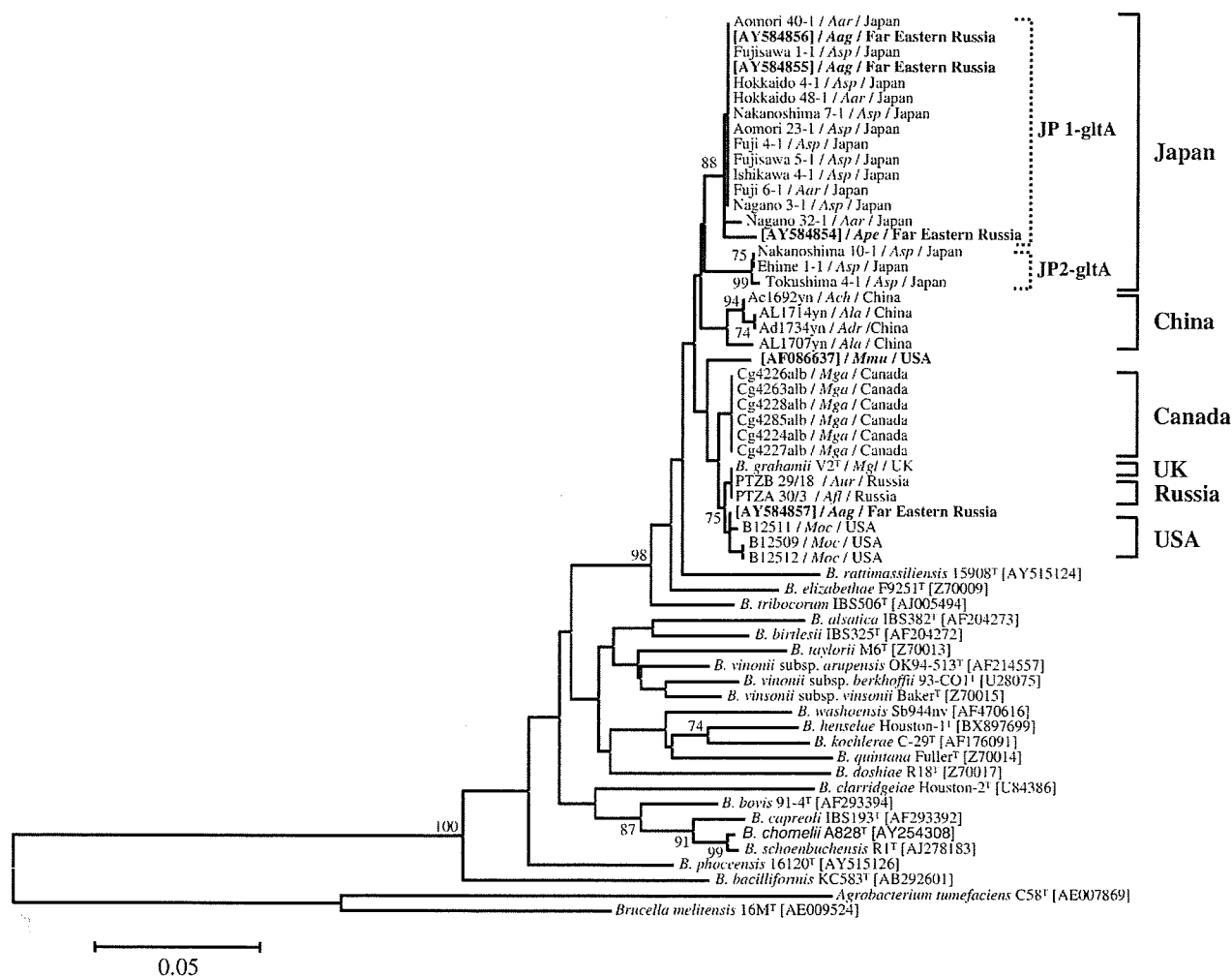


Figure 2 Phylogenetic tree of the 31 *B. grahamii* strains examined here and known *Bartonella* species constructed by the NJ method with Kimura's two-parameter distances method based on a part of *gltA* (312 bp). The GenBank accession numbers are indicated in parentheses. The phylogenetic tree includes partial sequences of *B. grahamii* from *Apodemus agrarius* and *A. peninsulae* in Far Eastern Russia (AY584854–AY584857) and from *Mus musculus* in the USA (AF086637). The derived host rodent species and country are shown after each slash. Bootstrap values (percentage of 1,000 replications) of

>70% are indicated at the node. The sequences of *Brucella melitensis* strain 16M and *Agrobacterium tumefaciens* strain C58 have been chosen as outgroups. The abbreviations of host species are as follows: *Aag*, *Apodemus agrarius*; *Aar*, *Apodemus argenteus*; *Ach*, *Apodemus chevrieri*; *Adr*, *Apodemus draco*; *Afl*, *Apodemus flavicollis*; *Ala*, *Apodemus latronum*; *Ape*, *Apodemus peninsulae*; *Asp*, *Apodemus speciosus*; *Aur*, *Apodemus uralensis*; *Mga*, *Myodes gapperi*; *Mgl*, *Myodes glareolus*; *Mmu*, *Mus musculus*, and *Moc*, *Microtus ochrogaster*

Japan 2 (i.e., Ehime 1-1, Nakanoshima 10-1, and Tokushima 4-1) that were derived from the southern part of Japan formed a large clade with the Chinese strains. Strains from Canada, the UK, Russia, and the USA formed a large clade as the American/European group. The strains from the USA were more closely related to those from the UK and Russia than to those from Canada.

All of the *B. grahamii* strains examined, except those from *Apodemus* mice, were grouped according to their host rodent genera (Fig. 1). Strains from Japanese and Chinese *Apodemus* mice belonged to the Asian group, whereas those from Russia were present in the American/European group.

Phylogenetic Analysis by *gltA*

The 31 strains were classified into 12 STs, and the sequence similarity among all 31 strains ranged from 96.5% to 100% (0–11 bp difference in 312 bp). The sequence similarities among the strains by country were 97.1–100% in Japan, 98.4–100% in China, 97.0–100% in Russia, 100% in Canada, and 99.4–100% in the USA, respectively. The sequence similarity in strains according to host rodent genera was 96.5–100% in *Apodemus* mice, 99.0–100% in *Myodes* voles, and 99.4–100% in *Microtus* voles.

The phylogenetic tree of *gltA* corresponded well with that of the concatenated sequences (Fig. 2). The strains

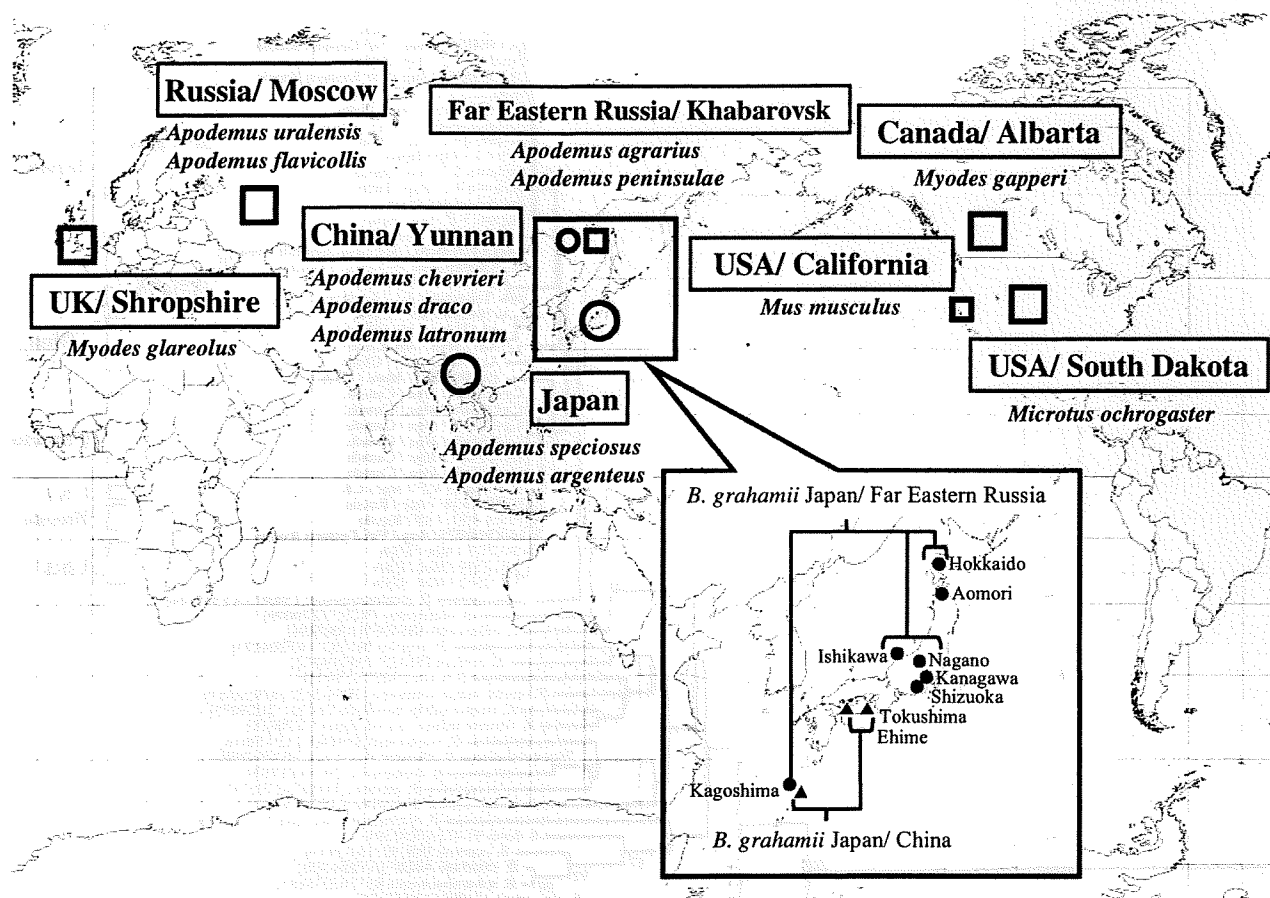


Figure 3 Geographic distribution of *B. grahamii* strains and their host rodent species. The areas where the *B. grahamii* strains of the Asian group and the American/European group have been isolated are indicated by open circles (○) and squares (□), respectively. The

distribution of two different *B. grahamii* groups in Japan (Japan/Far Eastern Russia and Japan/China) is indicated by a closed circle (●) and triangle (▲), respectively

formed clades according to the geographic locations where the rodents had been captured, although the Japanese strains formed two clades, namely JP1-gltA and JP2-gltA. Almost all Japanese strains were included in clade JP1-gltA; by contrast, clade JP2-gltA consisted of only three strains (i.e., Ehime 1-1, Nakanoshima 10-1, and Tokushima 4-1) that were isolated from the southern part of Japan. Three of the four sequences of *B. grahamii* (AY584854, AY584855, and AY584856) derived from two *A. agrarius* hosts and an *A. peninsulae* host in Far Eastern Russia were also clustered in clade JP1-gltA from Japan with 98.4–100% similarity. The remaining *B. grahamii* sequence (AY584857) from *A. agrarius* host in Far Eastern Russia formed a clade with the strains from *Microtus* voles in the USA, sharing 99.7% similarity. A sequence (AF086637) of *B. grahamii* derived from *Mus musculus* host captured in California, USA, was related to strains from Canada, the UK, Russia, and the USA with 97.4–98.4% similarity, but it was located outside the strains showing ancestral lineage.

As found for the concatenated sequences, all of the *B. grahamii* strains examined, except those from *Apodemus*

mice, were grouped according to their host rodent genera (Fig. 2). Two strains from *A. uralensis* and *A. flavicollis* hosts in Russia had sequences identical to that of a strain from a *Myodes* vole in the UK. The sequence (AY584857) of *B. grahamii* from *A. agrarius* host in Far Eastern Russia was closely related to those from *Microtus* voles in the USA (99.4–99.7% similarity).

Discussion

Previous studies have isolated *B. grahamii* from various rodents, including the genera *Myodes*, *Apodemus*, *Microtus*, *Mus*, and *Dryomys*, and have shown that this microorganism is widely distributed over all of the continents such as Asia [16, 29, 36], Europe [9, 15, 33], and North America [10, 17]. By MLSA, the 31 *B. grahamii* strains analyzed here showed genetic divergence and were classified into 10, 15, 12, 22, 14, and 16 STs for 16S rRNA, *ftsZ*, *gltA*, *groEL*, *ribC*, and *rpoB*, respectively. The diversity observed among *B. grahamii* strains from different parts of the world